IN-24
52355
P. 49

Effect of Open Hole on Tensile Failure Properties of 2D Triaxial Braided Textile Composites and Tape Equivalents

Timothy L. Norman, Colin Anglin, David Gaskin, and Mike Patrick

Effect of Open Hole on Tensile Failure Properties of 2D Triaxial Braided Textile Composites and Tape Equivalents

Timothy L. Norman, Colin Anglin, David Gaskin, and Mike Patrick
West Virginia University • Morgantown, West Virginia

June 1995

ABSTRACT

The unnotched and notched (open hole) tensile strength and failure mechanisms of two-dimensional (2D) triaxial braided composites were examined. The effect of notch size and notch position were investigated. Damage initiation and propagation in notched and unnotched coupons were also examined. Theory developed to predict the normal stress distribution near an open hole and failure for tape laminated composites was evaluated for its applicability to 2D triaxial braided textile composite materials. Four fiber architectures were considered with different combinations of braid angle, longitudinal and braider yarn size, and percentage of longitudinal yarns. Tape laminates equivalent to textile composites were also constructed for comparison. Unnotched tape equivalents were stronger than braided textiles but exhibited greater notch sensitivity. Notched textiles and tape equivalents have roughly the same strength at large notch sizes. Two common damage mechanisms were found: braider yarn cracking and near notch longitudinal yarn splitting. Cracking was found to initiate in braider yarns in unnotched and notched coupons, and propagate in the direction of the braider yarns until failure. Longitudinal yarn splitting occurred in three of four architectures that were longitudinally fiber dominated. Damage initiation stress decreased with increasing braid angle. No significant differences in prediction of near notch stress between textile and tape equivalents could be detected, but the strength of the correlations between measured and predicted stress were weak for textiles with large braid angle. Notch strength could not be predicted using existing anisotropic theory for braided textiles due to their insensitivity to notch.

Table of Contents

INTRODUCTION

Textile composite materials are receiving recognition as potential candidate materials for increasing damage tolerance of structures. Design for damage has become especially important because of increased expected service life of aircraft. Textile composites offer through-the-thickness reinforcement which should aid in preventing propagation of damage. In addition to expected high damage tolerance, textile composite architecture can be tailored to suit strength and stiffness requirements. They offer numerous options in material architecture, net shape geometry and enhance manufacturability of composites. Fibers and resins can be varied to optimize material performance. Typical textile composites include stitched, knitted, two-dimensional (2D) and three-dimensional (3D) woven and braided preform types. Although braider reinforcement increases damage tolerance, the performance of textile composites, e.g. strength, stiffness, toughness, is not understood. No methodology is currently available to predict the effect of notch for textile composite materials, even though open hole strength is often critical in design.

Limited studies are available in the literature to study the effects of notch in design of textiles. Curtis and Bishop [1] and Bishop [2] investigated notch sensitivity of woven and nonwoven Carbon-fiber reinforced plastics (CFRP). In their study, woven CFRP were compared to nonwoven laminates with equivalent (0,90), (±45) and (0,90, ±45) layups. (0,±45) laminates with ±45° layers replaced by woven layers were also studied. They found that notched woven laminates had reduced strength compared to nonwoven. For woven fibers at ±45° to the principal loading direction, the substitution of woven fiber for nonwoven material had little effect on the mechanical properties, and the material preserved its notch insensitivity in both woven and nonwoven forms. In addition, there were reductions in the stress concentration effects on the 0° fiber due to matrix cracking in the 45° layers. In a study by Naik et al. [3], the influence of stacking sequence was found to alter notched and unnotched strength and the failure mechanisms. Guidelines for optimum stacking sequence were reported.

Quasi-static tension and compression tests of thick cross-ply laminates of uniwoven AS/4 carbon fabric using a brittle matrix with and without stitching and a tough matrix material were conducted by Wolterman et al. [4]. Coupons with and without circular holes were tested to determine strength, modulus and failure strain. Tension and compression tests of open hole coupons indicated the presence of stress concentrations determined from failure stresses below predicted for unnotched laminate. The brittle matrix material failed with extensive longitudinal matrix cracking and fiber breakage throughout the section whereas the tough material failed at the hole due to fiber breakage. Results showed that the static mechanical properties were insensitive to matrix material because of high percentage of 0° fibers.

Material discontinuities including bolt, rivet, and open holes are critical factors in structural design [4]. At these locations, stress concentrations may cause cracks to occur which may propagate and result in overall catastrophic failure. The stress concentration factor (SCF) is the ratio of the maximum tensile hoop stress on the perimeter of the hole to the remote stress of the structure or test specimen. Use of the SCF in design of notched metallic alloys has been extensively characterized [5].

More recently, a study of in-plane mechanical properties of unidirectional composite tape laminates and 2D triaxially braided composites with notch (open and filled hole) was conducted [6]. In the referenced study, a very significant increase in open-hole and filled hole tension strength was observed for the braided textiles compared to their tape equivalent materials in tension. This increase did not hold true for compression properties, where the braid strengths were lower than for the laminates.

For composite laminates, the SCF itself is not an adequate measure of failure. Failure is based on a more complete description of stress near a hole [7]. Konish and Whitney [8] studied a load-free circular hole in an orthotropic, mid-plane symmetric composite tape laminate subjected to remote, uniaxial tension. An approximate solution to calculate the normal stress distribution adjacent to a circular hole in an infinite orthotropic plate was presented in the form of a polynomial. The approximate solution was compared with the complex elasticity solution where good agreement was found for a wide range of orthotropic stress concentration factors. It was concluded that the approximate solution is useful in assessing hole size effect on the notched strength of laminated orthotropic composite plates. It was also concluded that the approximate solution is a useful engineering design tool for optimizing laminate construction in the presence of a circular hole.

In this investigation, our overall goal was to determine how open hole effects failure in 2D braided textile composite materials under tensile loading. We tested four 2D braided textile composite architectures and their tape equivalents with the following objectives:

- determine notch sensitivity
- determine notch position sensitivity
- evaluate applicability of anisotropic theory for notch stress and failure prediction
- document damage initiation and propagation mechanisms
- compare strength and failure mechanisms of textile and tape equivalents

Specifically, 2D braided textile composite materials with variations in percentage of 0 degree fibers, percentage of braider yarn fibers and braid angle yielding four distinct architectures were investigated to determine the effect of notch on tensile strength. Notched and unnotched coupons were tested under static loading to failure to investigate the effects of hole size and hole placement

5

on ultimate failure stress. Damage initiation and progression to failure were also characterized using radiographs and photomicrographs of polished cross-sections at specific load intervals. The normal stress distribution measured from the notched coupon with three different open hole sizes were compared to predictions made from the approximate solution [8] for anisotropic materials. The point stress failure criteria [9,10] was also evaluated for prediction of failure in notched textiles. The approximate solutions were evaluated as potential design tools for 2D braided textile composites with open hole. Tape laminates equivalent to textile composites were constructed for comparison to the textile composites.

MATERIALS AND METHODS

<u>Materials and Specimen Preparation</u>

Four distinct triaxially braided materials were constructed from AS-4 fabric impregnated with Shell 1895 epoxy resin. Braid angle, yarn and braider size, percentage of longitudinal yarns, or volumetric proportion of longitudinal yarns to total yarn content, and braider angle varied. A description of the triaxial braid pattern (Fig. 1) is provided by Masters et al. [11]. The nominal layup configuration is given in Table 1 and the braid geometry is given in Table 2. In the tables, the following nomenclature has been adopted in order to describe the layup:

$$[0_{XX_k}/\pm\theta_{XX_k}]\ Y\%\ \text{Axial}$$

where XX indicates the yarn size, k indicates thousands and Y indicates the percentage of axial yarns in the preform. $[0_{6k}/\pm45_{15k}]12\%$ axial (LSS), $[0_{36k}/\pm45_{15k}]46\%$ axial (LLS), $[0_{30k}/\pm70_{6k}]46\%$ axial (SLL) and $[0_{75k}/\pm70_{15k}]46\%$ axial (LLL) plates were designed by NASA, braided by Fiber Innovations Inc. (Norwood, MA) and resin transfer molded by Boeing Aircraft Co. (Seattle, WA). Once fabricated, samples from each plate were used to determine fiber and resin content (Table 3) by Matrix Digestion (ASTM D-3171). The samples were digested using concentrated sulfuric acid and 30% hydrogen peroxide. The weight fractions were measured and volume fractions calculated based on density. The density used for AS-4 was 1.77 g/cm^3 and for the resin was 1.18 g/cm^3.

The 30.48 cm X 60.96 cm plates of nominal 3.175 mm thickness were machined into notched and unnotched coupons (Fig. 2). Coupons were taken from the plates without regard to position or architectural features. All dimensions were recorded. Three different coupon sizes were machined: 2.54 cm wide unnotched and notched, 5.08 cm wide notched and 10.16 cm wide notched. Notch sizes were chosen to maintain a coupon width to hole diameter equal to 4 (W/D = 4). This criterion yields hole sizes of 6.35 mm, 12.7 mm and 25.4 mm for 2.54 cm, 5.08 cm and

10.16 cm wide coupons, receptively. Gage length to width ratio (L/W) was 4 for 2.54 cm and 5.08 cm wide coupons and was 2.25 for 10.16 cm wide coupons. End tabs were cut from aluminum sheet and bonded to the ends of the coupons.

Tape laminates of equivalent material and layup geometry were designed at NASA Langley [12] and fabricated at West Virginia University. The equivalent laminates were made from AS4/3501-6 prepreg tape and were designed to have equivalent total areal weights, cross-ply angle equal to braid angle, unit ply consisting angle and longitudinal plies equivalent in areal weight to a 2D braided textile layer, equivalent number of unit plies (textile layers) and were designed to be as symmetric as possible (Table 4). Notched specimens of widths 2.54 cm and 10.16 cm were constructed as described previously. Notch sizes were 6.35 mm and 25.4 mm for the 2.54 cm and 10.16 cm wide specimens, respectively.

Specimens of all material types were mounted with strain gages to measure remote strain and near notch normal strain distribution (Fig. 3). For unnotched coupons, strain gages (MM CEA-13-500UW-120) were mounted in the center of each coupon. Remote strain gages for notched specimens (MM CEA-13-500UW-120) were mounted in the center of the coupon half way between the notch and the end tabs. These strain gages measured 4.6 mm in width and 12.7 mm in length which satisfied our criterion that the gage be at least as long as 2 times the unit cell height (Table 2). A total of five strain gages were mounted adjacent to the circular hole to measure the normal strain distribution. EA-13-015DJ-120 gages (0.38 mm x 0.51) were used for 2.54 cm width specimens and EA-13-031DE-120 gages (0.79 mm x 0.81 mm) were used for 5.08 cm and 10.16 cm width specimens. One gage was placed on each side of the specimen as close to the notch as possible, approximately 0.48 mm from center of the gage to the hole edge (x-R) for the 2.54 cm specimen (Fig. 3, Table 5). A third gage was placed approximately 1.3 mm away from the notch for 2.54 cm width specimen. Distances were greater for the 5.08 and 10.16 cm specimens (Table 5). A fourth gage was placed mid-way between the hole and the specimen edge and a fifth gage was placed at 2.54 mm from the specimen edge. Strain gages (EA-13-031DE-120) were also placed at 45° and 90° to the normal of the load direction as close to the hole as possible (Fig. 3).

Experimental Procedure

Tests were conducted using the test matrix outlined in Table 6 as a guide. Coupons were clamped between the grips of a servo-hydraulic testing machine (Interlaken, Minneapolis, Minn). An extensometer with a 2.54 cm gage length was mounted to the coupon on the opposite side of the coupon adjacent to the strain gage. This allowed comparisons between the strain gage and the

7

extensometer. Coupons were subjected to a static load at a displacement rate of 0.254 mm/min (0.01 in/min) while load, stroke and extensometer and strain gage strain were recorded. There were three different coupon groups for braided textile and tape equivalents (Table 6): Load to failure, nondestructive evaluation (NDE) and destructive evaluation coupons. Load to failure and near notch strain coupons were loaded until catastrophic failure occurred and used as failure allowables. Notched and unnotched NDE coupons measuring 2.54 cm in width were loaded to designated load levels, removed from the testing machine and radiographed. The failure loads of these coupons were not included in the average of load to failure coupons. Coupons with widths measuring 5.08 cm and 10.16 cm were radiographed at specified intervals while mounted in the machine using a portable X-ray machine available at Langley Research Center. During hold times, loading was reduced to avoid creep. Notched and unnotched destructive evaluation coupons were loaded to 50%, 75% and 95% of the failure stress. Longitudinal, transverse and cuts perpendicular to the braider yarns were removed from coupons with a diamond blade sectioning saw (Fig. 4). The sectioned composites were embedded in an epoxy-resin mount and polished using a Buehler Ecomet 2 grinder-polisher (Buehler Inc., Lake Bluff, ILL.). Photomicrographs were taken using an Olympus (Lake Success, N.Y.) dissecting research microscope.

Method of Analysis

Near Notch Strain Predictions

The presence of notches in a laminate creates the problem of stress concentrations around the cutouts. The approximate normal stress distribution away from the hole can be obtained through the use of the extended isotropic solution [7, 8, 9]:

$$\frac{\sigma(\xi)}{\sigma_o} = 1 + \frac{\xi^{-2}}{2} + \frac{3\xi^{-4}}{2} - \frac{K_T - 3}{2}(5\xi^{-6} - 7\xi^{-8}) \tag{1}$$

where $\xi = x/R$ which is the distance from the center of the hole divided by the hole radius, $\sigma(\xi)$ is the stress at position ξ, and σ_o is the remote stress. This approximate solution is obtained by adding sixth and eighth order terms to the exact solution proposed by Leknitski [7], requiring that stress concentration factor be obtained at the hole boundary and that force resultants of both the exact and approximate anisotropic stress distribution are equal. Assuming the plate infinite when compared to the hole size

$$\sigma_{\theta\theta}\big|_{r=R} = f(\theta)\sigma_o \tag{2}$$

where R is the hole radius and $f(\theta)$ is defined as

8

$$f(\theta) = \frac{E_\theta}{E_1} \left[-(\cos^2 \phi - (q+k)\sin^2 \phi)q\cos^2 \theta + ((1+k)\cos^2 \phi \right.$$

$$\left. -q\sin^2 \phi)\sin^2 \theta - k(1+q+k)\sin\phi\cos\phi\sin\theta\cos\theta \right] \qquad (3)$$

where ϕ is the load angle ($\phi = 0$, along longitudinal direction), θ is the angle at which $\sigma_{\theta\theta}$ is measured (measured from longitudinal) and E_θ, k, p and q depend on the material laminate properties E_1, E_2, G_{12} and v_{12} as follows:

and

$$\frac{1}{E_\theta} = \frac{\sin^4\theta}{E_1} + \left(\frac{1}{G_{12}} + 2\frac{v_{12}}{E_1} \right) \sin^2\theta \cos^2\theta + \frac{\cos^4\theta}{E_2} \qquad (4)$$

where

$$k = \sqrt{p + 2q}$$

$$p = \frac{E_1}{G_{12}} - 2v_{12}$$

$$q = \sqrt{\frac{E_1}{E_2}}$$

The stress concentration factor, K_t, is the maximum value of $f(\theta)$. A computer program for calculating laminate stresses and strains using lamination theory was modified to include the extended isotropic solution.

Point Stress Failure Theory

Applicability of existing notch failure theory developed for anisotropic materials was tested for textile composites. Using the point stress failure theory developed by Whitney and Nuismer [9], a characteristic distance, d_o, is calculated from experimentally measured notched (σ_N) and unnotched (σ_{UN}) strengths. The characteristic distance is the distance between the edge of the notch and some point away from the notch where the stress is equal to the (unnotched) strength. According to Whitney and Nuismer [9, 10],

$$\sigma_N = \frac{2\sigma_{UN}}{2 + \xi_o^{-2} + 3\xi_o^{-4} - (K_t - 3)(5\xi_o^{-6} - 7\xi_o^{-8})} \qquad (5)$$

where

$$\xi_o = \frac{a + d_o}{a}$$

9

with a equal to the hole radius. d_0 was calculated using the same stress concentration factor calculated for the near notch strain predictions described above along with the notched and the unnotched strength.

RESULTS

Notch Sensitivity

Net failure stress of notched and unnotched textile and tape equivalent coupons are shown in Figs. 5-7 and Table 7. The net failure stresses have been normalized to 60% fiber volume fracture according to the following equation:

$$\sigma_{net} (corr) = \sigma_{net} *0.6/v_f$$

where σ_{net} is the measured net stress, v_f is the measured fiber volume fraction and σ_{net} (corr) is the measured net failure stress adjusted to 60% fiber volume fraction. Notch sensitivity is evaluated based on net failure stress because we wanted to assess the sensitivity of the notch alone, and not the reduction in stress associated with a decrease in cross-sectional area.

LSS textiles (Fig. 5) exhibited a small difference in notched and unnotched strengths and indicated slightly greater strength than the tape laminates. LLS tape laminates exhibit significant notch sensitivity (Fig. 5) at small notch sizes but the sensitivity decreases with increasing notch size. The LLS textile appears relatively notch insensitive and has a small decreasing strength with increasing notch size. SLL tape exhibited greater notch sensitivity than the textile at smaller notch sizes (Fig. 6). The textile and tape equivalent have approximately the same notch strength at all notch sizes but the tape has higher unnotched strength. LLL tape exhibited significantly greater notch sensitivity than the LLL textile (Fig. 7). The textile and tape 1" hole specimens have approximately the same strength. In summary, in three of four architectures (LLS, SLL, LLL), the tape laminates exhibited greater notch sensitivity than the textiles. Even though the strength of the tape equivalents was greater initially, the strengths of the notched textiles and tape equivalents were approximately the same for the largest notch size tested. In the other case (LSS), the notch sensitivity was roughly equivalent.

Statistical Analysis of Failure Data
Strengths

Statistical analysis was used to detect significant differences in strength of the different architectures. The data were analyzed using two way ANOVA. The design variables were the materials (tape and textile), architectures (LSS, LLS, SLL and LLL) and hole size (0, 0.25", 0.5"

and 1.0"). All combinations were not included in the test matrix (i.e. 0.5" holes were not tested for tapes, and all possible combinations of architectures were not tested) making it difficult to attribute reason for significance among all combinations, but were enough to make the following comparisons:

- Strengths of tape equivalents were greater than textiles when averaged across all architectures and hole diameters.
- The difference between tape and textile strengths (when averaged over all hole sizes) is not the same for all architectures, with the difference being greater for the LLL and LSS architectures in that order.
- For the textiles, there was a significant difference in the mean strengths between architectures ($p < 0.00001$) averaged across all hole diameters and between hole diameters ($p < 0.00001$) when averaged across all architectures.
- For the textiles, there was significant interaction between architecture and hole diameter meaning that the difference in mean strengths between hole sizes changes significantly from one architecture to another.
- For the textiles, the difference between mean strengths of the unnotched, 0.25" and 0.5" diameter holes averaged across all architectures are not significantly different, but the difference between the mean strengths of unnotched, 0.25" and 0.5" diameter holes are significantly different from the mean strength of the 1.0" diameter hole .

Strength Ratio

Using a similar statistical analysis, the strength ratios (notched strength to unnotched strength) were analyzed and optimum combinations of hole size for the braids were determined (Fig. 8). The strength ratio

- for the 0.25" hole LLL was less than that for the other architectures, but the difference was not significant.
- for the 0.5" hole LSS was less than that for the other architectures but significant ($p < 0.05$) for LLL only.
- for the 0.5" hole LLL was greater than that for the other architectures but significant for the LSS only.
- for the 1.0" hole SLL was less than that for the other architectures but significant for the LLS only.

These optimum combinations provide a guideline for design of notched textile composites with the four architectures tested.

Notch Position Sensitivity

The coefficient of variation (COV), defined as the standard deviation divided by the mean net failure stress, is shown in Figs. 9 and 10 for the LSS and LLS architectures, respectively. It was proposed that COV could be used as an indicator of notch position sensitivity (i.e. if notched coupons exhibited larger COV than unnotched coupons for holes that are randomly placed, notch

11

position sensitivity is indicated). For the textiles alone, the COV's indicated that the LSS textile architecture was not sensitive to notch position whereas the LLS textile architecture was. This criteria was applied to the tape equivalents, which exhibited a similar trend. Because tape laminates should not be sensitive to notch position (due to microscopic homogeneity), we concluded that variation of COV observed between architectures was a function of material geometry and not notch position sensitivity. Thus, our criteria was not valid measure of notch position sensitivity.

Near Notch Strain Predictions

Material properties for the tape equivalent laminates were calculated using lamination theory (Table 8) and used along with equation (3) to calculate the stress concentration factor (Fig. 11) for tape and textile coupons. The curves are symmetric and have a period of $180°$. The LLL and SLL have the same stress concentration factor (due to their layup geometry) and yielded the highest value of 3.71 followed by the LLS of 3.34 and the LSS of 2.4. The stress concentration factors are negative for θ less than approximately $35°$. The stress ratio calculated from equation (1) provides an indication of the strain gradient away from the notch (Fig. 12). Shown also in the figure for comparison are the strain ratio determined from Moire' interferometry [13].

Measured strain-stress curves at each gage location are shown in Fig. 13a. The front and back gages have the highest strain and have approximately the same magnitude. Strain of the second gage is smaller than the gages nearer to the hole (front and back gages). The edge gage and remote gages have approximately the same magnitude and are the smallest strains of the gages mounted normal to the load direction. The $45°$ gage strain is small and positive while the 90 degree gage strain is large and negative as expeced.

Remote strain measured from gage 6 (Fig. 3) of the textile and tape equivalent materials was multiplied by the stress ratio corresponding to the position (ξ) of each gage location (Table 5) from which predicted strain-stress curves were generated. A typical comparison of measured and predicted stress-strain curves is shown for the textile front (1), back (2) and second (3) strain gages (Fig. 13b). Measured strains from edge and remote gages are also shown. The slopes of the measured and predicted strain-stress curves for all materials and specimen sizes were compared using statistical analysis. The analysis of these data was the ANOVA for a split plot design in which the whole plots were: material (braided textile or tape equivalent), architecture (LSS, LLS, SLL and LLL), specimen width (one inch or four inches). The subplots were locations: front, back, second or middle. The variable was the difference between observed and predicted slopes. None of the sources caused significant variability in the variable of analysis. Hence, there are no

significant differences between the means of textiles and tape equivalents, nor between the means of the four architectures, etc..

An analysis of the slopes for observed vs. predicted was also performed (Figs. 14 and 15) for each braid angle. The R^2 value of the figure is the fraction of variability in measured slope (y-axis) values which is explained by the linear relationship with predicted slope (x-axis). Results for LSS and LLS textile architectures indicated very good fits of the lines to the data (Fig. 14a). The trend line should be 0.00 + 1.00x, and both approximate that quite closely. The fit is a little better for the equivalent laminated material (Fig. 14b) (seen in larger R^2), but the differences weren't significant. Correlations for the slopes of SLL and LLL architectures (Fig. 15a) were not as good as LLS and LSS, but were within an acceptable range. Measured and predicted slopes correlated better for the SLL and LLL tape equivalents (Fig. 15b) than the braided textiles, with the R^2 for the tape equivalents roughly equal to that of the LLS and LSS architectures, but the differences between tape and textile were not significant. These data suggests that the strength of predictions of near notch stress decreases with increasing braid angle for textiles.

Failure Prediction

Using the stress concentration factor calculated for the near notch strain predictions (Fig. 11) along with the notched and the unnotched strength, equation (5) was used to calculate d_o. Shown in figures 16-19 are the notched failure data normalized by the unnotched data for the four architectures tested along with the theoretical predicted strength generated from calculated d_o. As can be seen, textiles are less notch sensitive than tape equivalents as indicated for the large values of d_o for the textiles and by the area under the stress ratio vs. hole radius curves (the textiles exhibit significantly greater d_o values and greater area under the curves than the tape equivalents). The values of d_o for the textiles are generally much larger than those for the tape equivalents.

Damage Initiation and Propagation Mechanisms

Damage initiation stress of 1" notched and unnotched textiles coupons was determined using the radiographs of specimens taken at small intervals of loading (Fig. 20, Table 9). The initiation stresses were normalized to the ultimate failure stress of the notched and unnotched coupons. The data in the figure indicates that damage initiation level and the difference between notched and unnotched initiation stress decreases with increasing braid angle.

Two dominate damage mechanisms were observed in notched textiles: braider yarn cracking and longitudinal yarn splitting. Longitudinal yarn splitting occurred near the notch for

13

longitudinally dominated architectures and was associated with shear lag effect. Braider yarn cracking occurred along the coupon edge (in notched and unnotched) and along the notch edge. Crack density increased with little to no cracking observed in the longitudinal yarns until failure.

Radiographs for notched textile and tape equivalent coupons at 75% of failure stress are shown in Fig. 21. These radiographs show cracking along the braid angle in all textile and tape equivalents and longitudinal cracking in the longitudinally dominated architectures (LLS, SLL and LLL, tape and textiles). A 45° section of an LSS notched coupon at 75% of failure stress shows that cracking along the braider yarn angle is braider yarn splitting and occurs through the thickness (Fig. 22), similar to cracking observed along the coupon edge. A transverse section of a notched LLS textile coupon (Fig. 23) shows the location of the longitudinal crack identified at the hole edge (Fig. 21b). The cracking is identified as longitudinal yarn splitting. In the tape equivalent coupons (Fig. 24), the longitudinal crack was within the 0° plies. The cracks in the 0° plies of tape equivalents propagated to the interface between the angle plies and 0 degree plies and then propagated to the hole edge, indicted by the shaded region in the radiographs (Fig. 21b,c,d). In the textiles, however, the longitudinal cracks propagated to the yarn edge, and in some cases to an adjacent yarn, where they were suppressed from further propagation.

Radiographs taken at progressive intervals indicated the cracking initiates in the braider yarns within the notch and along the edge of unnotched coupons and propagates along the braid angle. Crack density increases along the braider yarns until fracture (Fig. 25). A pronounced fracture line occurs along the 45° braider yarn in the LSS (braider dominated) coupons. Fracture in the other three longitudinally dominated architectures tended to occur normal to the load direction by without a pronounced fracture line and encompasses a larger area. After failure, cracking was frequently observed in the braider yarns and was seldom found in longitudinal yarns (Fig. 26). Longitudinal and braider yarn delaminations were frequently observed in the failure region. Longitudinal yarn cracking was observed in the failure regions but seldom away from the failure region or before failure. Similar failure mechanisms were observed in all architectures. The notched coupons fractured similar to unnotched coupons.

DISCUSSION

The objective of this study was to investigate the effect of notch on tensile strength and failure mechanisms on 2D braided textile composite materials. Four distinct textile architectures and their tape equivalents were investigated. Notched and unnotched coupons were tested under static loading to failure to investigate the effects of hole size and hole placement on ultimate tensile failure stress. Damage initiation and propagation mechanisms were also characterized. The normal

14

strain distribution measured from the notched coupon with three different open hole sizes were compared to predictions made from an approximate solution and failure criteria developed for tape composites was also evaluated for textiles.

The textile composites exhibited notch insensitivity. In three of four cases, there was no reduction in strength for small notch sizes, and a relatively small reduction for larger notch sizes when compared to tape laminates. Even though the unnotched tape laminates where stronger than the unnotched textiles, after an open hole was placed in the coupons, the materials had roughly equivalent strengths. This is important since often open hole strength influences design, and, consequently, the textile structure can be designed for strength with less notch "knock-down" factor currently considered for tape laminates. Textile composites structures can be designed for other desirable features, e.g. net shape fabrication, damage tolerance, with less penalty for open hole strength.

In the case of the LLL architecture, the 0.5" notch exhibited less notch sensitivity than the 0.25" notch, inconsistent with the other data sets. Figure 27 shows the number of longitudinals for each net section specimen width. The number longitudinals for unnotched (1.0" net width), 1.0" notched (0.75" net width), and 2.0" notched (1.5" net width) were determined from microscopic inspection of cross sections from the tested specimens. The number of longitudinals for the 4" notched (3.0" net width) were determined form extrapolation of the curve. The number of longitudinals are shown plotted against the net strength in Figure 28, suggests that there is a competing sensitivity between the notch and too few longitudinals. The data suggests that for the LLL architecture, the minimum specimen net section width should be approximately 1.5", as this is when the peak failure load was achieved. After this width, the notch sensitivity becomes more apparent by a significant decrease in failure stress with increasing notch size whereas before this size, it appears that there is a decrease in net failure stress due to too few longitudinals.

An evaluation of the approximate solution for calculation of normal stress distribution of textile composite materials with an unloaded open hole was made. The theory tested in this study was developed for a load free hole in an orthotropic plate with mid-plane symmetry subjected to the remote uniaxial tension. The textile composite is anisotropic with architectural variations across the specimen width and through the thickness due to axial and braider fiber bundles. The longitudinal and transverse bundles are spaced across the width, undulate as they are braided and nest with bundles from adjacent layers. Thus, it might be expected that large differences would occur between measured and predicted normal strain distribution near the notch in braided textiles as compared to tape equivalents. This did not occur. The approximate theory was equally effective for the braided textile and tape laminates. For these materials, the theory was able to predict the measured strain-stress slope regardless of material, architecture, specimen width and hole size or

gage location. For the ±70 degree braid angle coupons (SLL and LLL), the comparisons between measured and predicted were acceptable but weak in comparison to the tape equivalent laminates. These data suggest that accuracy of predictions of near notch strain decreases with increasing braid angle for textiles.

The applicability of theory developed to predict failure in tape composite for textiles did not have a favorable outcome for textiles. Characteristic distances calculated for the theory were unreasonable and physically unrealistic for the textiles but are within an acceptable range for the tape equivalents. We concluded that the theory was not applicable for the textiles due to their notch insensitivity. Failure methodologies developed by other investigators [14] should also be evaluated.

Damage initiation and propagation mechanisms in unnotched and notched coupons were the same for all architectures with the exception of off-axis dominated architecture (LSS), which did not experience longitudinal yarn cracking. Cracks initiated in the braider yarns through the thickness and propagated along the braider yarns increasing in density until fracture. Crack propagation mechanisms for notched and unnotched coupons were the same. The longitudinally dominated architectures developed longitudinal yarn splitting at the notch associated with shear lag that propagated in the load direction with increasing load. Damage initiation stress decreased with increasing braid angle.

The notched textile composites exhibited delamination suppression. It has been well documented that tape laminates have low damage tolerance due to weak lamina interface. This was demonstrated in our study radiographically and in photomicrographs (Figs. 23 and 24). The longitudinal cracking in 0° plies of tape laminates that occurred near the notch due to shear transfer, or shear lag, propagated to the 0/±45 interface and then propagated in the form of delamination to the hole edge (Fig. 24). Radiographs and photomicrographs of the textile indicated that longitudinal cracking near the notch due to shear was found in the longitudinal yarns and propagated to the outside perimeter of the yarn and infrequently into an adjacent yarn, but in most cases did not propagate beyond its own interface, as there is no "ply interface" for propagation to occur. This may contribute to the apparent notch insensitivity observed in this study. On a larger scale, delamination is a common failure mechanisms for large cutouts in composite structure. Our results suggest that use of textile composites may be beneficial for composite structure with cutouts that are large were delamination plays a role in failure.

Results from this investigation suggest an inherent weakness in the braider yarns of the triaxial braided textile composites tested in this study. We found that crack initiation and propagation along the braider yarns is the driving mechanism leading to failure. The braider yarn crack density increases significantly with loading suggesting that crack propagation within the

16

braiders continues with relatively little resistance. The braider yarns move above and below the longitudinal tows as they are braided across the width of the coupon. Thus, as crack density increases, the longitudinal yarns are surrounded by a number of points of stress concentration caused from the cracked braider yarns. We hypothesize that as the stress reaches some critical value, the stress concentration at the crack tip of the braider yarn causes the longitudinal yarns to fracture, resulting in the coupon failure along the braid direction. Our experimental observations support our hypothesis. The braider yarn is a unidirectional composite with high fiber volume fracture and apparently little damage tolerance. The travel of the braider along or near to the 45° maximum shear plane of the coupon makes the braider a likely location for damage to occur in tensile loading. Results of this study suggest that improving the damage resistance of the braider yarn may delay fracture onset of the textile composites evaluated in this study.

CONCLUSIONS

In summary, the following conclusions have been made concerning the materials tested in this study:

- Generally speaking, unnotched tape equivalents are stronger than braided textiles but exhibited greater notch sensitivity.
- Notched textiles and tape equivalents have roughly the same strength at large notch sizes.
- Notch position sensitivity could not be tested by coefficient of variation.
- No significant differences in prediction of near notch strain between textile and tape equivalents could be detected for all architectures, but the strength of the correlations was weak for textiles with large braid angle.
- Notch strength could not be predicted using existing anisotropic theory for braided textiles.
- Damage initiation stress decreases with increasing braid angle.
- Braider yarn cracking dominates failure process.
- Near notch longitudinal cracks associated with shear lag occur in longitudinally dominated architectures.

ACKNOWLEDGMENT

thank Dr. Stanley Wearden, Department of Mathematics and Statistics, West Virginia University, for statistical support.

REFERENCES

[1] Curtis, P. T. and Bishop, S. M., "An Assessment of the Potential of Woven Carbon Fibre-Reinforced Plastics for High Performance Applications," *Composites,* Vol. 15, No. 4, October, 1984, pp. 259-265.

[2] Bishop, S. M., "Strength and Failure of Woven Carbon Fibre Reinforced Plastics of High Performance Applications," *Textile Structural Composites,* Edited by Tsu-Wei Chou and Frank K. Ko, Elsevier, 1989, New York.

[3] Naik, N. K. Shembekar, P. S. and Verma, M. K., "On the Influence of Stacking Sequence on Notch Sensitively of Fabric Laminates," *Journal of Composite Materials,* Vol. 24, 1990, pp. 838-852.

[4] Wolterman, R. L., Kennedy, J. M. and Farley, G. L., "Fatigue Damage in Thick, Cross-Ply Laminates with a Center Hole," *Composite Materials: Fatigue and Fracture, Fourth Volume, ASTM STP 1156,* W. W. Stinchcomb and N. E. Ashbaugh, Eds., American Society for Testing and Materials, Philadelphia, 1993.

[5] Peterson, R. E., Stress Concentration Factors, John Wiley, New York, NY, 1974.

[6] Minguet, P. J. and Gunther, C. K., "A Comparison of Graphite/Epoxy Tape Laminates and 2-D Braided Composites Mechanical Properties," NASA Contractor Report 4610, July, 1994.

[7] Lekhnitskii, J. E. 1963. Theory of Elasticity of an Anisotropic Body. San Francisco, CA: Holden-Day.

[8] Konish, H. J. and Whitney, J. M., "Approximate Stresses in an Orthotropic Plate Containing a Circular Hole," J. Composite Materials. 9:157-166, 1975.

[9] Whitney, J. M. and Nuismer, R. J., "Stress Fracture Criteria for Laminate Composites Containing Stress Concentrations," J. Composite Materials, 8:253-265, 1974.

[10] Ghasemi, N. and Chou, T.W., "A Model for the Prediction of Compressive Strength reduction of Composite Laminates with Molded-In Holes," *J. Composite Materials,* Vol. 24, pp. 236-255, 1990.

[11] Masters, J. E., Foye, R. L., Pastore, C. M. and Gowayed, Y. A. 1993. Journal of Composites Technology and Research, 15:112-122.

[12] Informal communication of C.C. Poe at NASA Langley.

[13] Ifju, Peter, presentation at the 1994 Textile Composites symposium at NASA Langley Research Center, Hampton, Va., Dec. 6-8, 1994.

[14] Poe, C.C., Jr., "Fracture Toughness of Fibrous Composite Materials," NASA Technical Paper 2370, November, 1984.

Table 1. 2D Triaxial Braid Configuration.

Material	Braid Code	Braid Pattern	Braid Yarn Size (No. of fibers)	Percent 0° Yarns (%)	0° Yarn Size (No. of fibers)
$[0_{6k}/\pm45_{15k}]$ 12% Axial	LSS	0/±45	15K	12	6K
$[0_{36k}/\pm45_{15k}]$ 46% Axial	LLS	0/±45	15K	46	36K
$[0_{30k}/\pm70_{6k}]$ 46% Axial	SLL	0/±70	6K	46	30K
$[0_{75k}/\pm70_{15k}]$ 46% Axial	LLL	0/±70	15K	46	75K

Table 2. 2D Triaxial Braid Geometry.

Material	Braid Code	Braid Yarn Spacing Yarns/cm. (Yarns/in)	0° Yarn Spacing, Yarns/cm. (Yarns/in)	Unit Cell Size Width x Height cm (in)	Number of Braid Layers
$[0_{6k}/\pm45_{15k}]$ 12% Axial	LSS	2.60 (6.60)	1.81 (4.60)	1.052 x 0.526 (0.414 x 0.207)	5
$[0_{36k}/\pm45_{15k}]$ 46% Axial	LLS	2.56 (6.50)	1.81 (4.60)	1.052 x 0.526 (0.414 x 0.207)	3
$[0_{30k}/\pm70_{6k}]$ 46% Axial	SLL	4.80 (12.2)	1.65 (4.2)	1.163 x 0.211 (0.458 x 0.083)	4
$[0_{75k}/\pm70_{15k}]$ 46% Axial	LLL	2.68 (6.8)	0.906 (2.3)	2.106 x 0.381 (0.829 x 0.15)	3

Braid yarn spacings were taken from J. Masters, Jan. - March, 1993 Progress Report. Unit Cell sizes were taken from J. Masters, July 21-23, 1993 Working Group Meeting. Braid geometry is based on a nominal thickness of 0.25 inch.

Table 3. Laminate Fiber and Resin Content

Material	Braid Code	Density g/cm^3	Fiber Weigth (%)	Resin Volume (%)	Fiber Volume (%)	Tape Eq. Fiber Volume (%)
$[0_{6k}/\pm45_{15k}]$ 12% Axial	LSS	1.56	69.9	39.8	60.6	67.3
$[0_{36k}/\pm45_{15k}]$ 46% Axial	LLS	1.54	68.4	41.3	58.8	69.4
$[0_{30k}/\pm70_{6k}]$ 46% Axial	SLL	1.56	69.9	38.6	61.4	63.4
$[0_{75k}/\pm70_{15k}]$ 46% Axial	LLL	1.56	71.6	36.9	63.2	65.1

Table 4. 2D braided textile and tape equivalent laminates.

2D Braided Material		Tape Equivalent Laminate
Type	Braid Material	Layup Geometry
LSS	$[0_{6k}/\pm45_{15k}]12\%$	$(45/-45)_2/0/(45/-45)_3/0/(-45/45)_3/0/(-45/45)_2$
LLS	$[0_{36k}/\pm45_{15k}]46\%$	$45/-45/0_3/(45/-45)_2/0_4/(-45/45)_2/0_3/-45/45$
SLL	$[0_{30k}/\pm70_{6k}]46\%$	$(70/-70/0_2)_2/0/70/-70/-70/70/0/(0_2/-70/70)_2$
LLL	$[0_{75k}/\pm70_{15k}]46\%$	$70/-70/0_3/(70/-70)_2/0_4/(-70/70)_2/0_3/-70/70$

21

Table 5. Strain gage locations for textile and tape equivalent laminates.

Gage	Specimen Width					
	2.54 cm (1.0 in)		5.08 cm (2.0 in)		10.16 cm (4.0 in)	
	x-R (mm)	$\xi = x/R$	x-R (mm)	$\xi = x/R$	x-R (mm)	$\xi = x/R$
1	0.48	1.152	0.91	1.144	0.91	1.072
2	0.48	1.152	0.91	1.144	0.91	1.072
3	1.30	1.408	4.62	1.728	4.88	1.384
4	5.18	2.632	9.70	2.528	19.12	2.506
5	2.13[1]	3.328	2.54[1]	3.6	2.54[1]	3.8
7[2], 8[3]	0.48	1.152	0.91	1.144	0.91	1.072

[1] measured from coupon edge

[2] gage at 45° to load direction

[3] gage at 90° to load direction

Table 6. Proposed test matrix for each architecture. The test plan for tape equivalents does not include 5.08 cm wide notched specimens.

Coupon Type	Total Count	Load to Failure	Radiographs	Destructive Sectioning
2.54 cm Wide Unnotched	12	6	3	3
2.54 cm Wide Notched	15	6	3	3
5.08 cm Wide Notched	5	5	3	0
10.16 cm Wide Notched	5	5	3	0

Table 7. Net failure stress and failure strain. Stress is normalized to 60% fiber volume fraction and standard deviations are indicated by parenthesis.

Specimen Type	Unnotched Failure strain (με)	Net Failure Stress (Ksi)			
		Unnotched	1" Notched	2" Notched	4" Notched
LSS					
Tape	13,450 (91.4)	54.4 (5.7)	41.1 (3.6)	-----	36.5 (1.0)
Textile	11,996 (305)	50.7 (2.8)	51.9 (0.6)	42.6 (1.9)	38.3 (1.0)
LLS					
Tape	12,653 (505)	123.2 (10.4)	95.3 (13.7)	-----	78.4 (11.2)
Textile	9,632 (308)	94.1 (4.2)	92.7 (10.3)	89.9 (6.8)	77.1 (5.5)
SLL					
Tape	13,432 (1463)	121.3 (21.1)	109.3 (16.1)	-----	66.1 (5.5)
Textile	12,402 (875)	108.1 (10.9)	106.3 (10.4)	99.6 (5.3)	64.8 (2.4)
LLL					
Tape	12,813 (1820)	117.0 (25.0)	98.9 (12.0)	-----	62.7 (10.8)
Textile	10,400 (1431)	77.7 (13.6)	68.9 (14.3)	82.5 (7.3)	55.0 (1.1)

Table 8. Predicted mechanical propeties for textile composites using lamination theory and tape equivalent layup geometry. Measured values ± standard deviations for textiles are indicted in the brackets.

Material Property	LSS	LLS	SLL	LLL
E_1 (Msi) [measured]	4.98 [5.00 ± 0.04]	10.68 [10.25 ± 0.32]	9.91 [10.00 ± 0.49]	9.91 [9.17 ± 0.77]
E_2 (Msi)	3.48	3.47	9.22	9.22
G_{12} (Msi)	4.60	3.16	1.76	1.76
v_{12}	0.75	0.69	0.15	0.15

Table 9. Damage intiation stress and strain for 1" wide notched and unnotched textile composite specimens.

Specimen Type	Initiation Strain (με)	Initiation Stress (Ksi)	Percent Mean Failure stress (%)
LSS			
Notched	2,515	12.6	24
Unnotched	3,702	19.4	38
LLS			
Notched	2,360	24.4	27
Unnotched	5,640	58.2	63
SLL			
Notched	1,441	21.0	20
Unnotched	2,599	25.9	24
LLL			
Notched	686	9.5	20
Unnotched	1,043	10.48	14
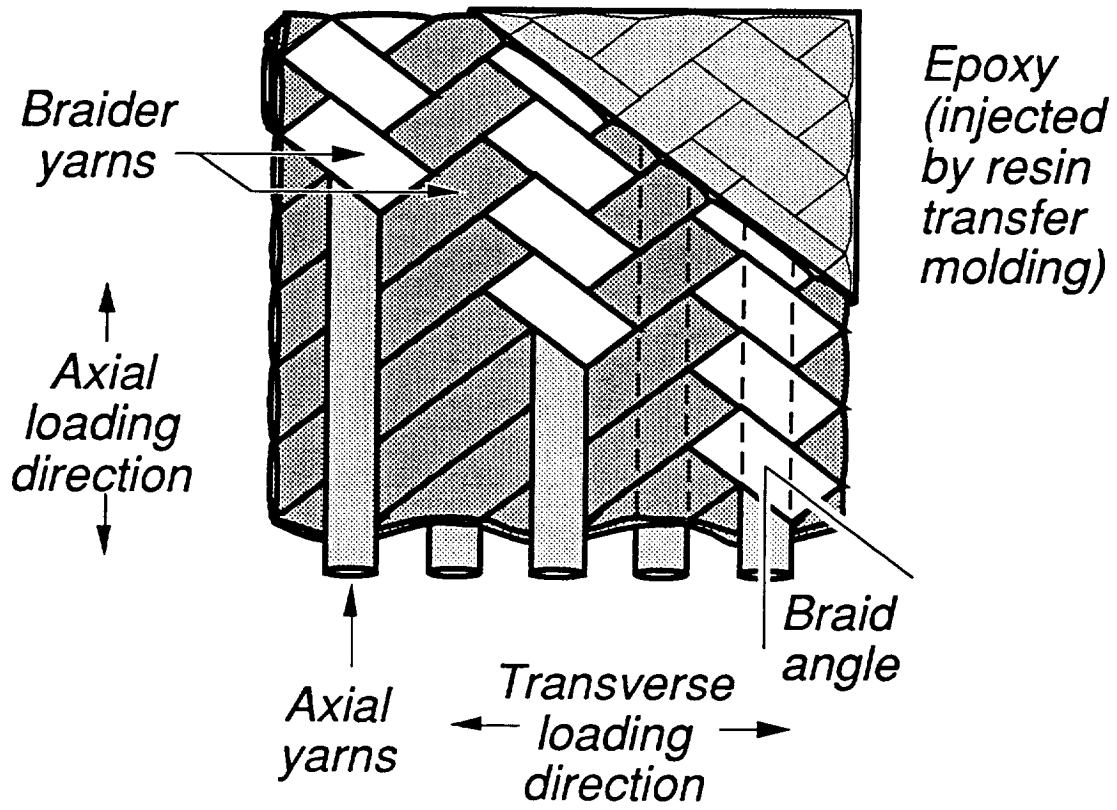
Figure 1. Triaxial braid configuration [13].
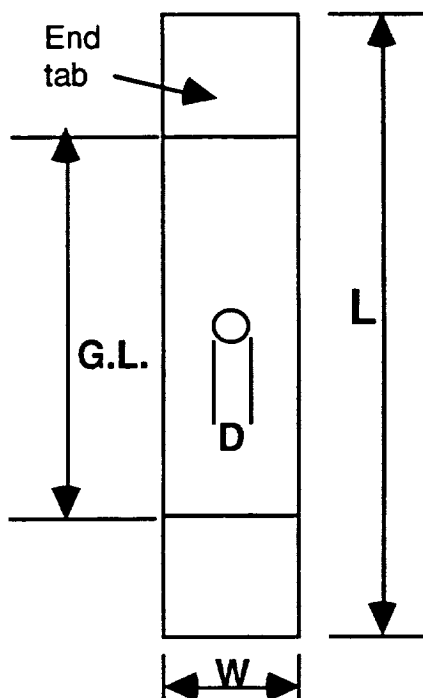
Specimen Width (cm)	L (cm)	G.L. (cm)	D (mm)	G.L./W	W/D
*2.54	15.24	10.16	6.35	4	4
5.08	27.94	20.32	12.7	4	4
10.16	30.48	22.86	25.4	2.25	4

* dimensions same for unnotched specimens

Figure 2. Notched specimen dimensions.

Front and back gages

Front gages

1 - Front hole gage
2 - Back hole gage
3 - Second hole gage
4 - Middle gage
5 - Edge gage
6 - Remote gage
7 - 45 gage
8 - 90 gage
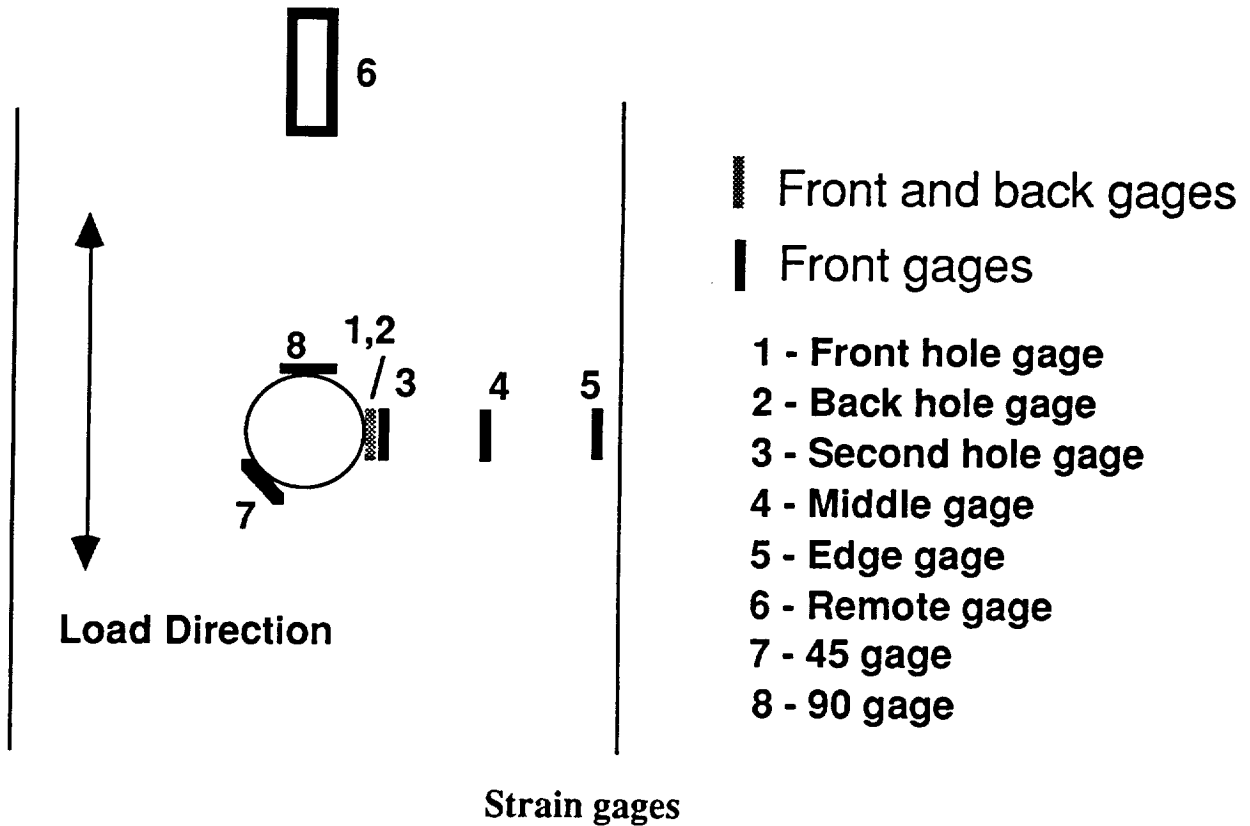
Strain gages

Remote Gage 6
MM CEA-13-500UW-120 (12.7 mm x 4.6 mm)

Gages 1-5, 2.54 cm (1") Specimen
EA-13-015DJ-120 (0.38 mm x 0.51 mm)

Gages 1-5, 5.08 cm (2") and 10.16 cm (4") specimen
EA-13-031DE-120 (0.79 mm x 0.81 mm)

Gages 7 and 8 all specimens
EA-13-031-DE-120 (0.79 mm x 0.81 mm)

Figure 3. Strain gage locations for near notch strain measurement.
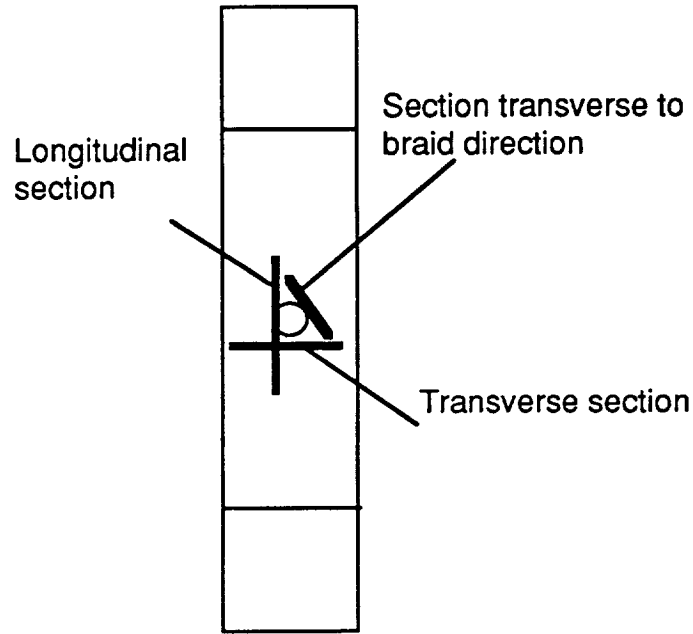
Figure 4. Orientation of sections taken for photomicrographs.
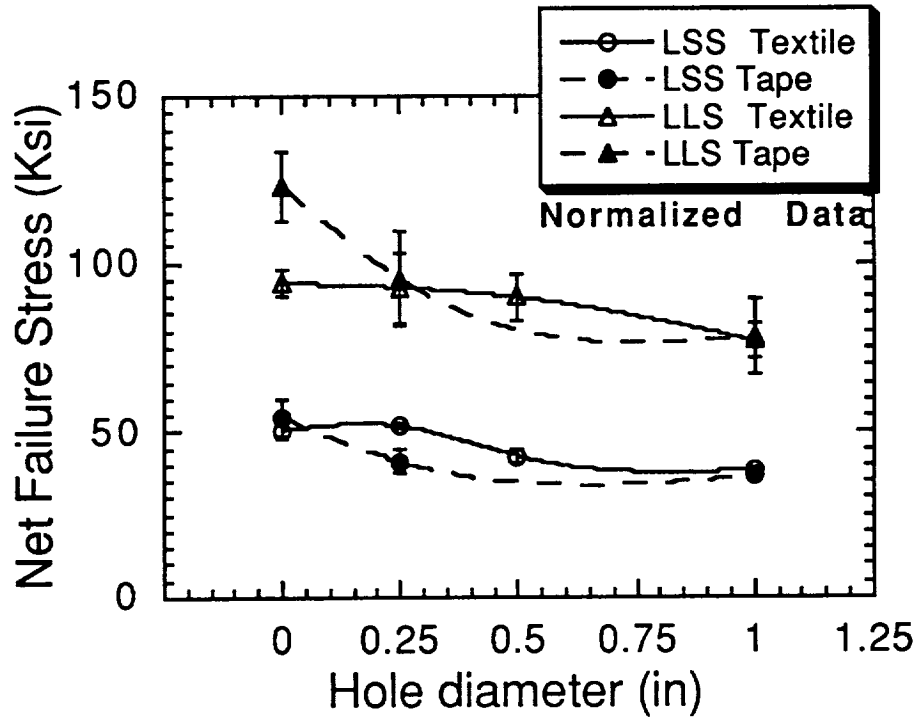
Figure 5. Net failure stress of LSS and LLS textile and tape equivalents.
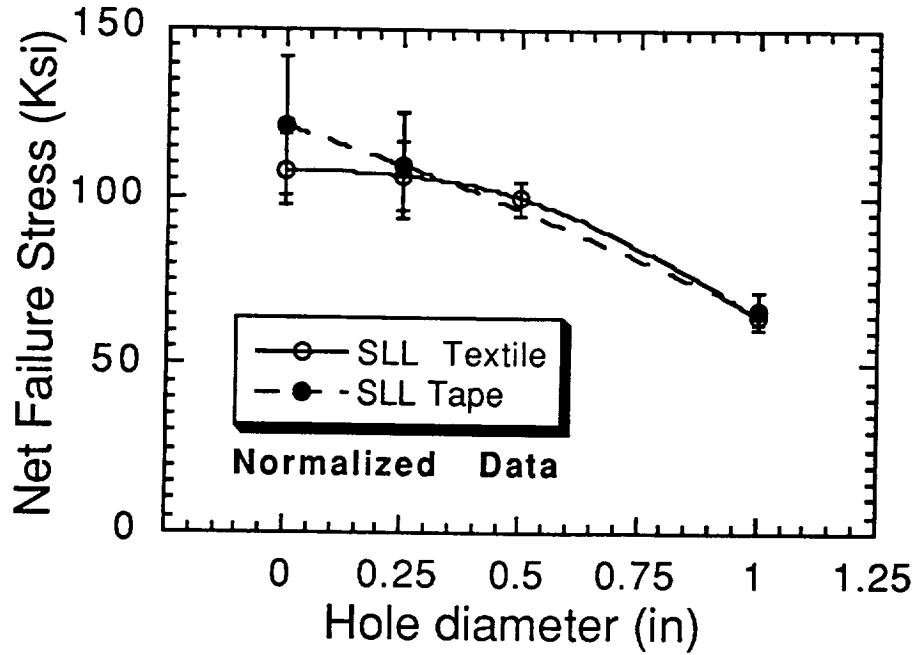
Figure 6. Net failure stress for SLL textile and tape equivalents.
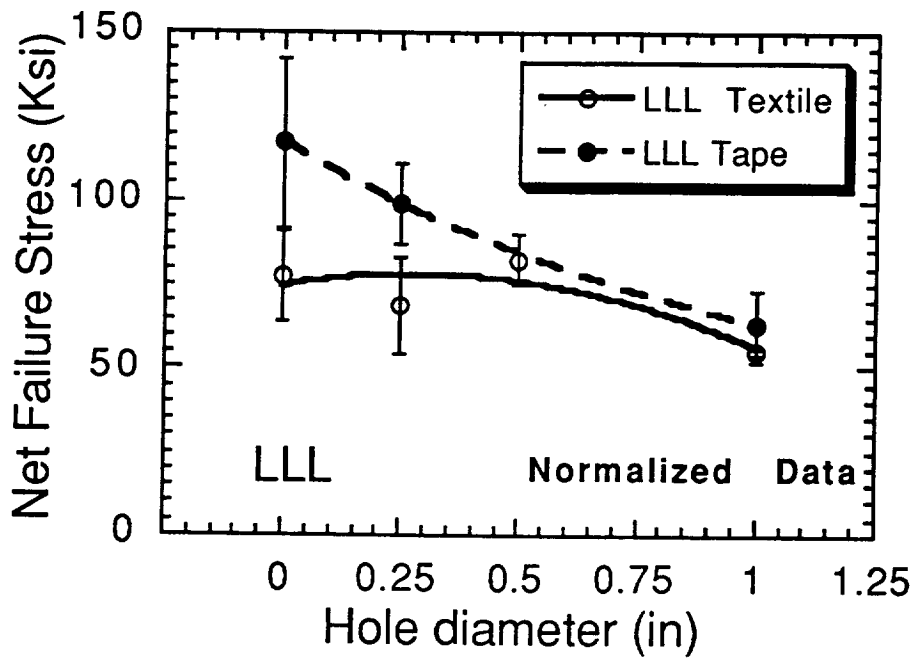
Figure 7. Net failure stress for LLL textile and tape equivalents.
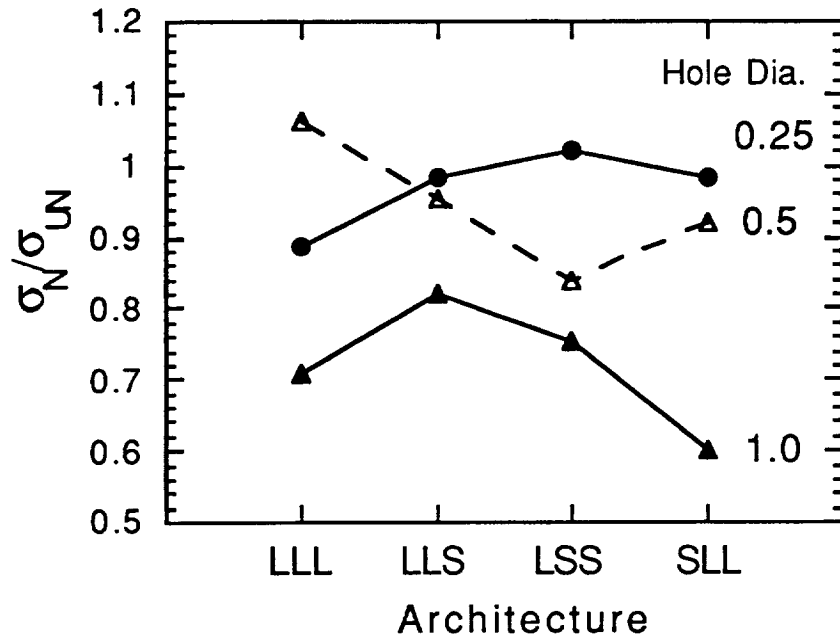
Figure 8. Architecture effect on hole size.
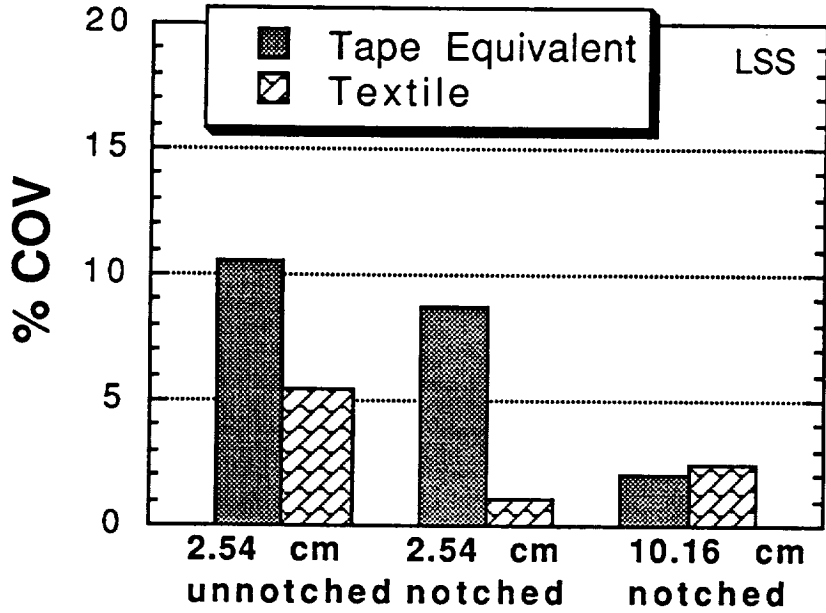
Figure 9. Coefficient of Variation (COV) of LSS textile and tape equivalents.
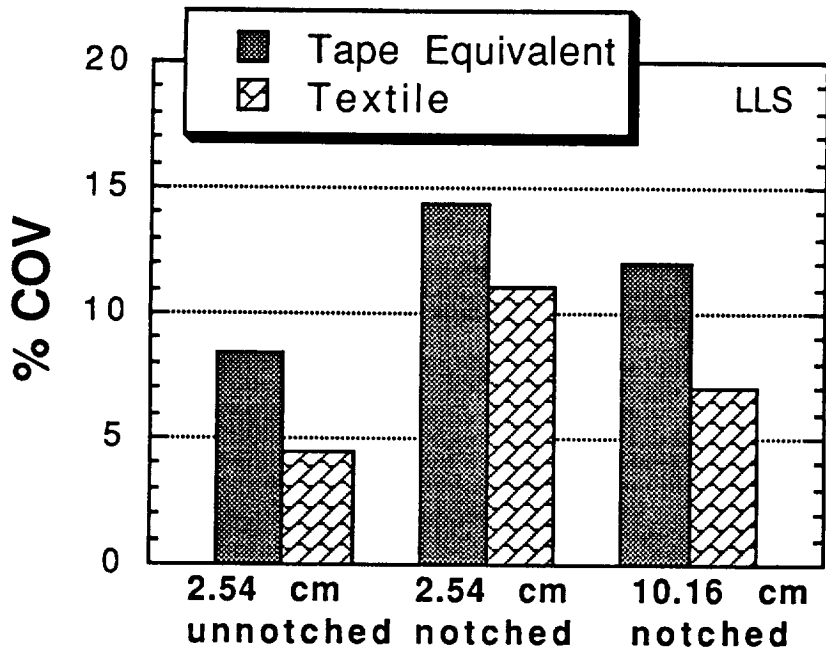
Figure 10. Coefficient of Variation (COV) fof LLS textile and tape equivalents.
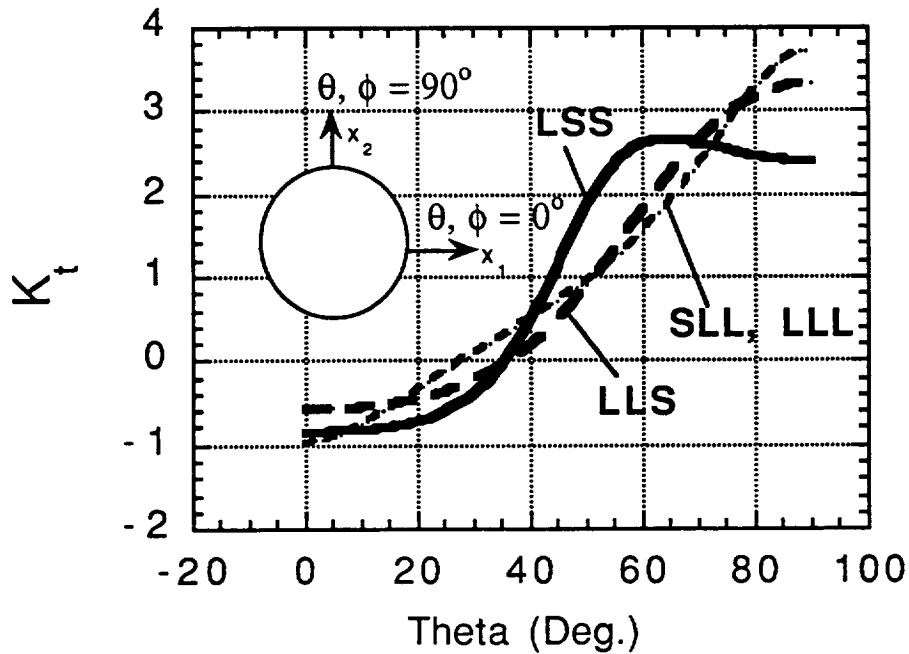
Figure 11. Stress concentration factor around a notch calculated from approximate theory for anisotropic materials using equivalent laminate material properties. The load and longitudinal direction corresponds to $\theta = 0°$.
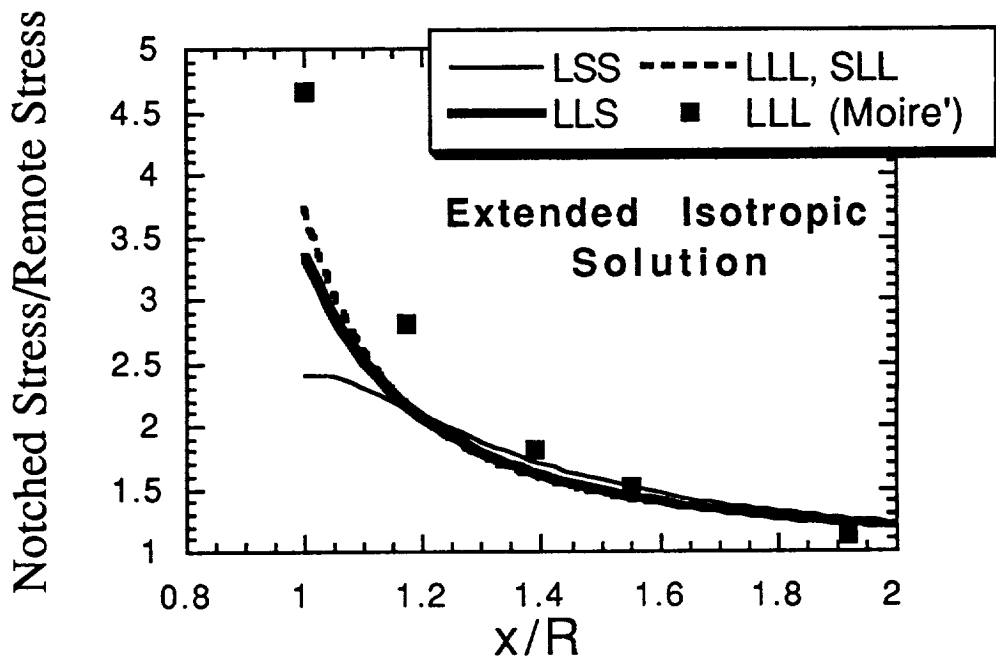
Figure 12. Approximate variation in strain away from notch in textile and tape equivalents. x/R = 1.0 corresponds to the hole edge. Results obtained from Moire' interferometry are also shown for comparison [13].
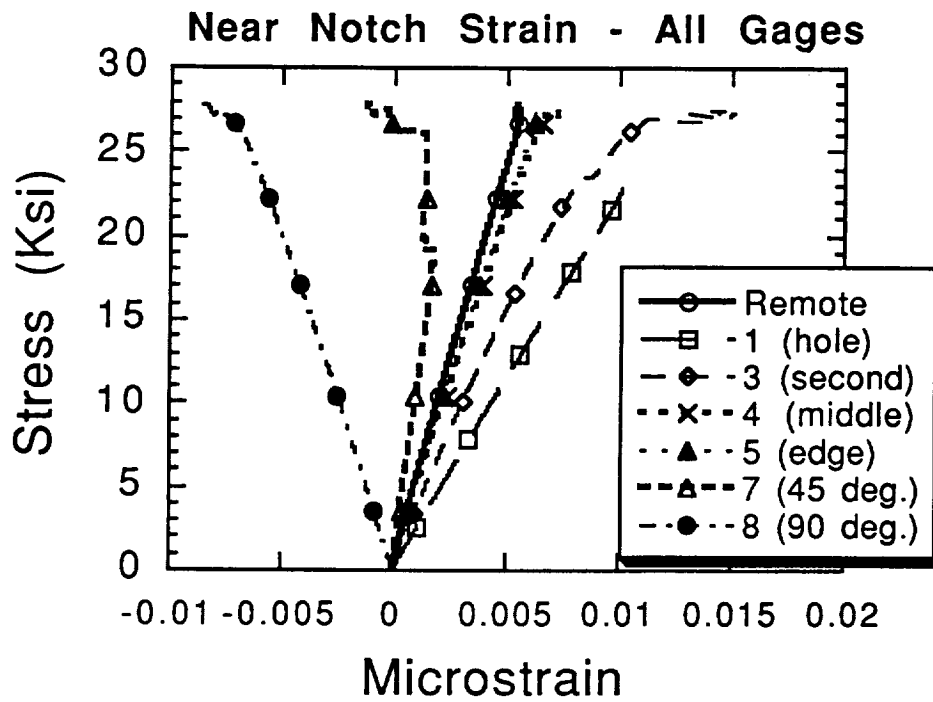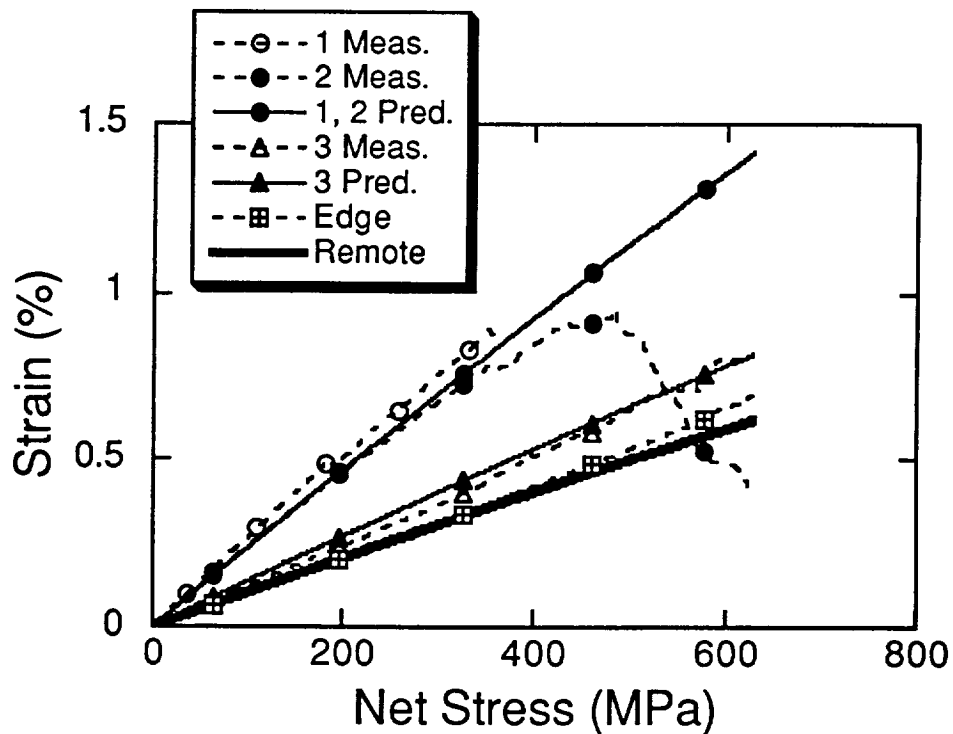
Figure 13. (a) Measured and (b) measured and predicted near notch strain. Predictions are made from remote gage strain multiplied by the approximate stress concentration factor.
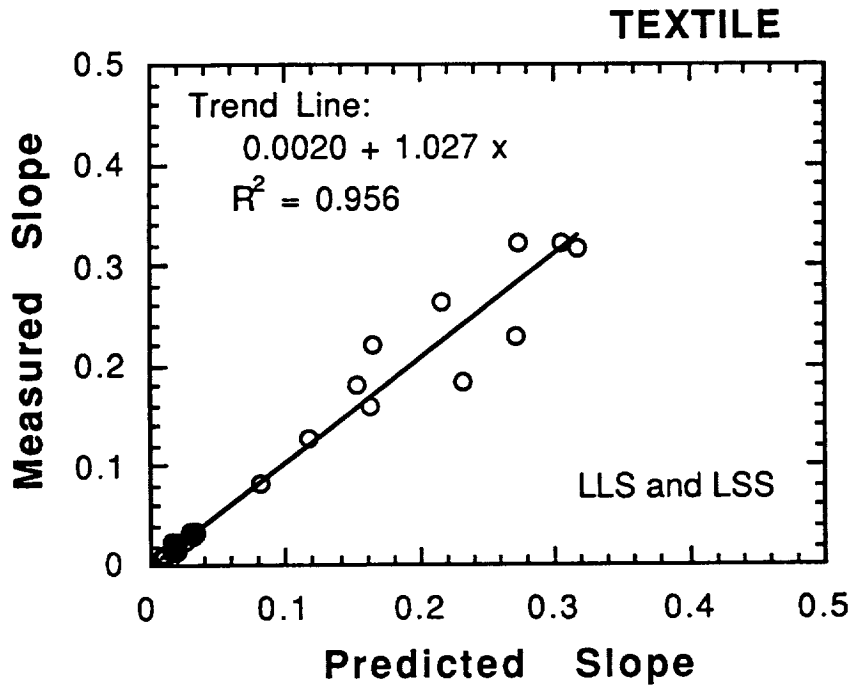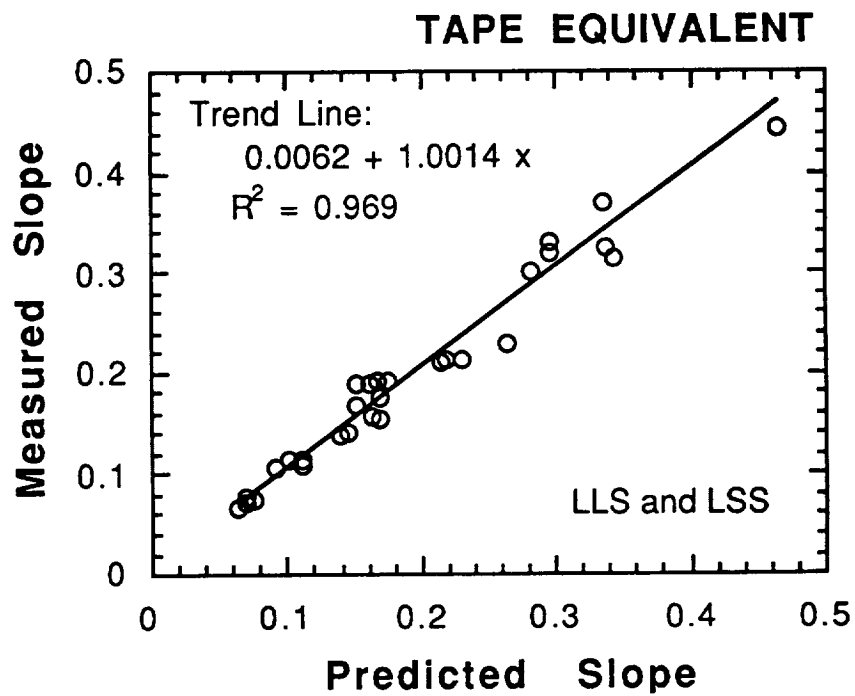
Figure 14. Correlation betweeen measured and predicted near notch strain-stress slope for a) textile and b) tape equivalent LLS and LSS architectures.

TEXTILE

Trend Line:
0.0462 + 0.7395 x
R^2 = 0.603

SLL and LLL

Measured Slope

Predicted Slope

a)

TAPE EQUIVALENT

Trend Line:
0.0328 + 0.8254 x
R^2 = 0.942

SLL and LLL

Measured Slope

Predicted Slope

b)
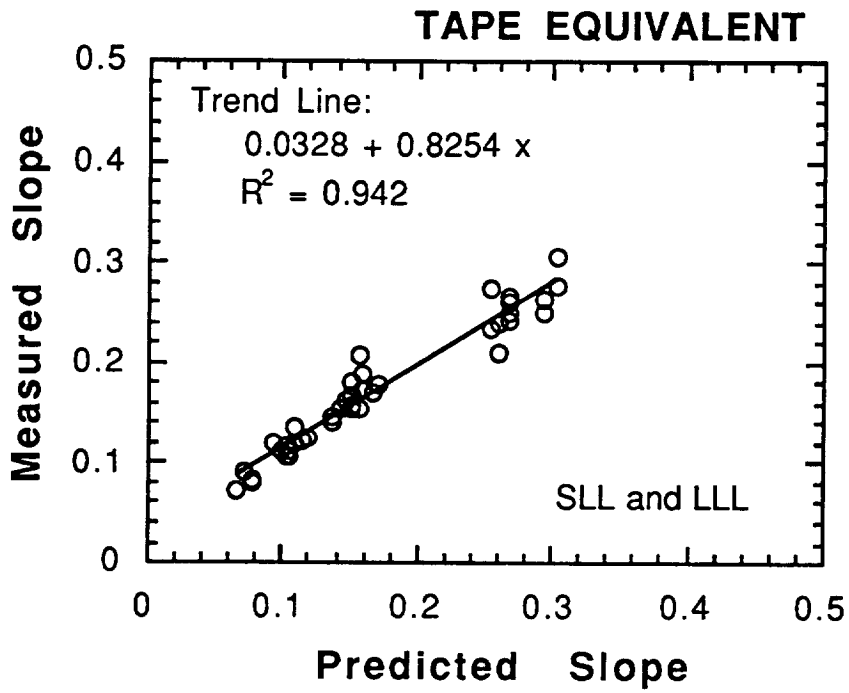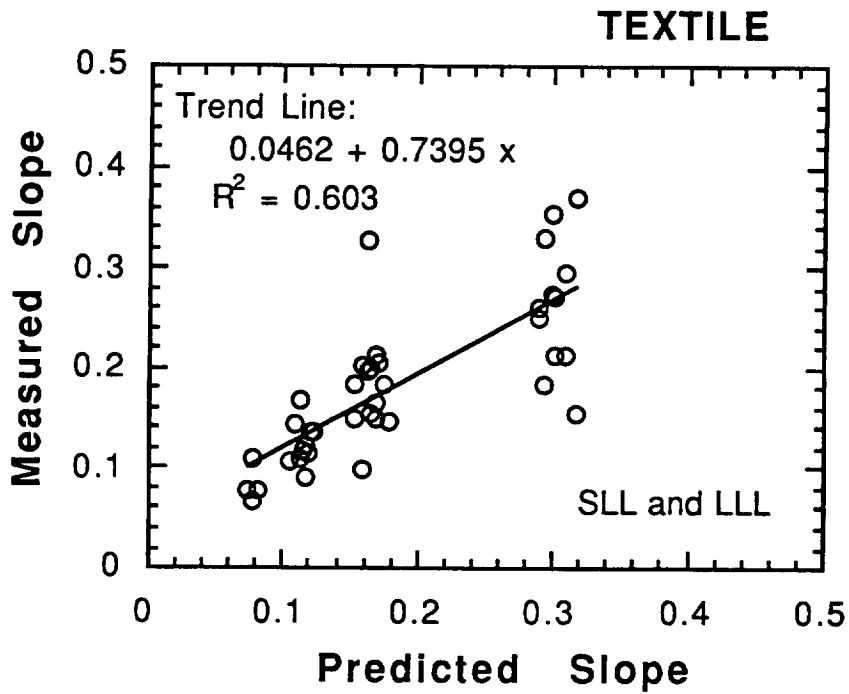
Figure 15. Correlation betweeen measured and predicted near notch strain-stress slope for a) textile and b) tape equivalent of SLL and LLL architectures.

35
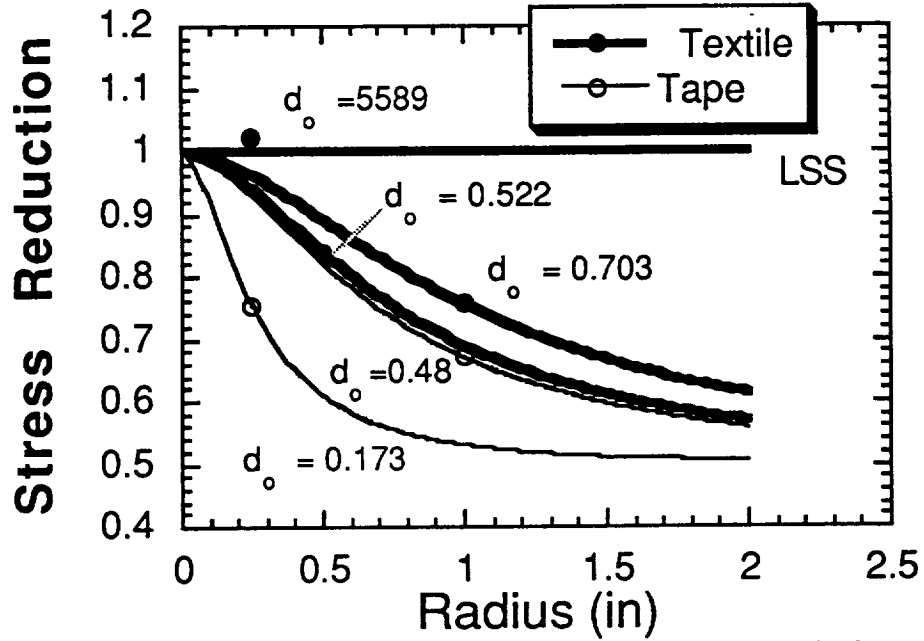
Figure 16. Point stress failure criteria for LSS textiles and tape equivalents.
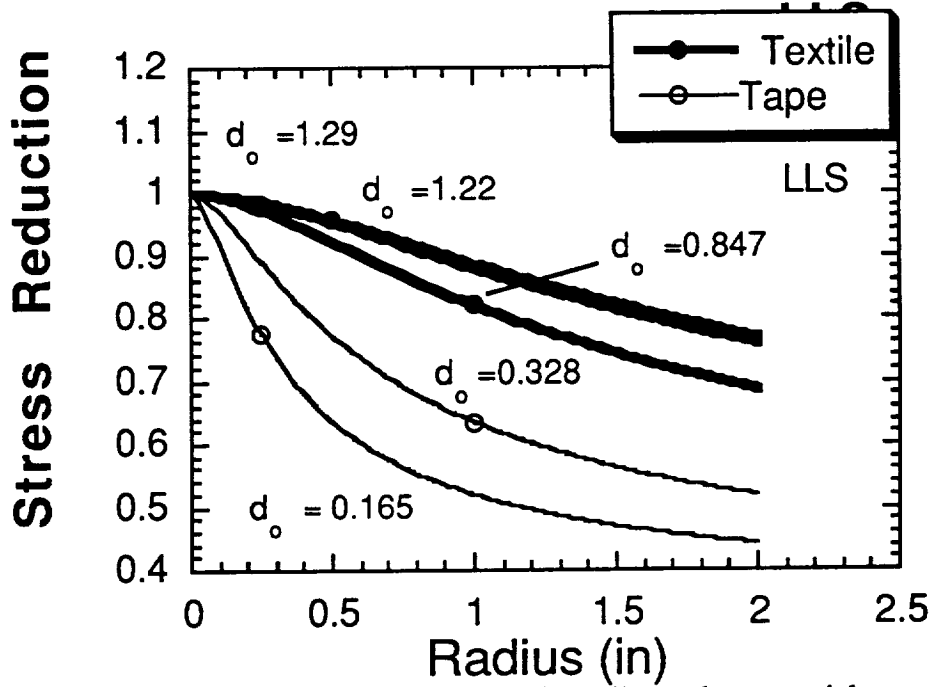
Figure 17. Point stress failure criteria for LLS textiles and tape equialents.
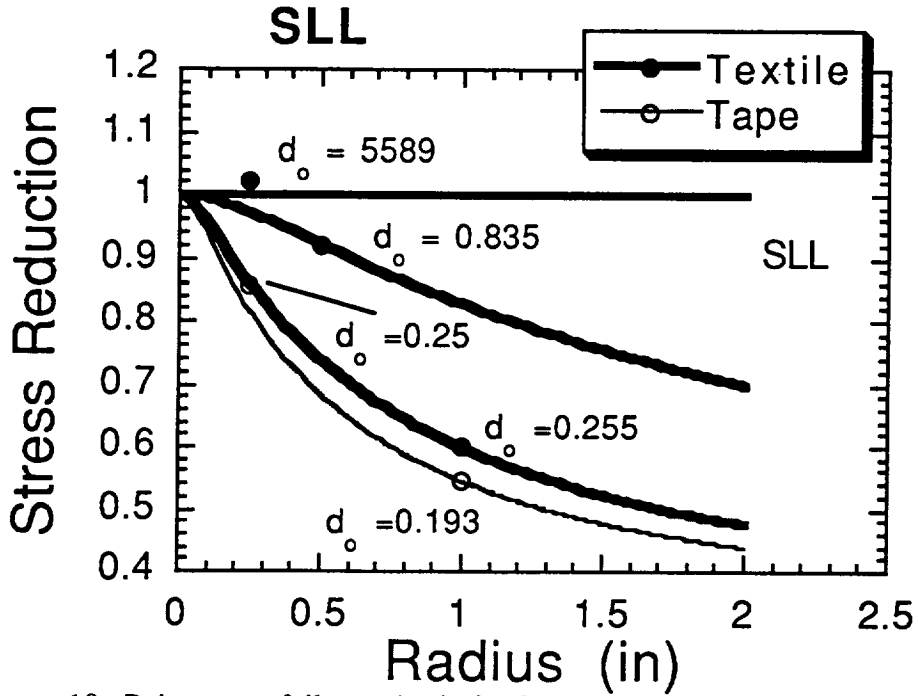
Figure 18. Point stress failure criteria for SLL textiles and tape equialents.
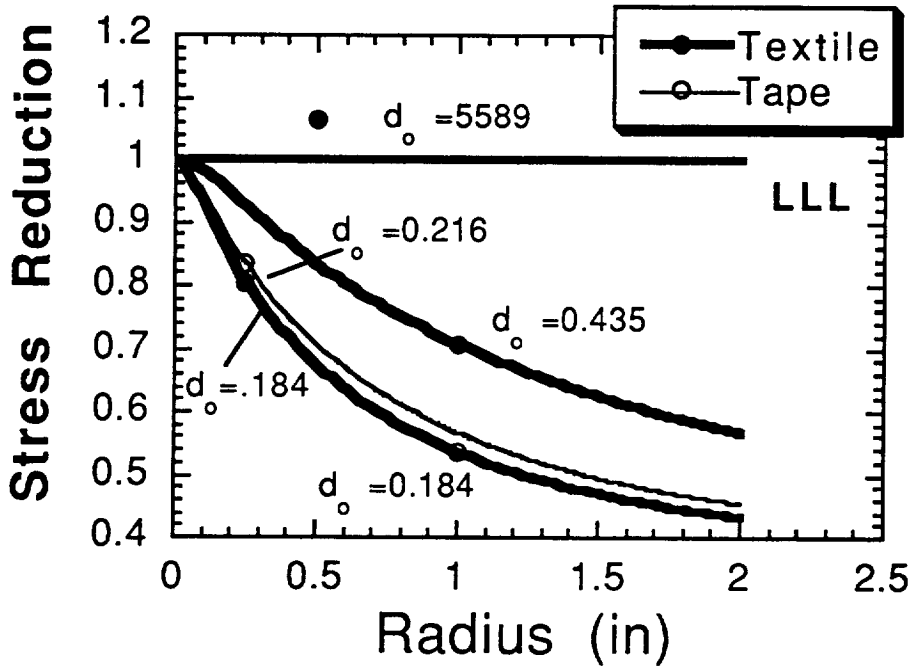
Figure 19. Point stress failure criteria for LLL textiles and tape equialents.
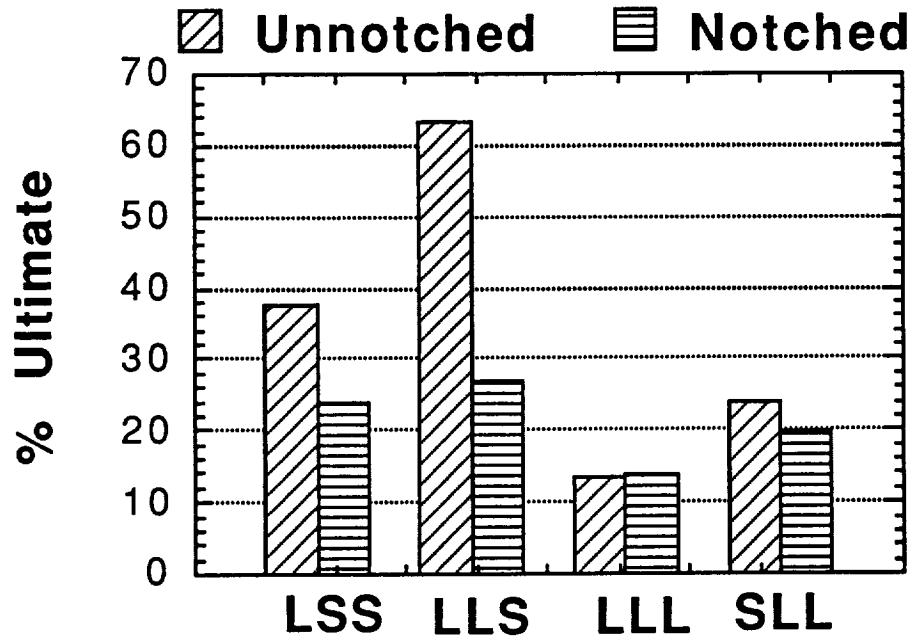
Figure 20. Damage initiation stress for 1" wide textile coupons expressed as % ultimate.

LSS
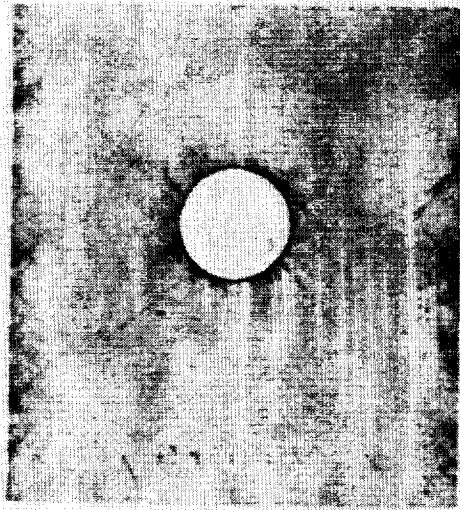
Tape
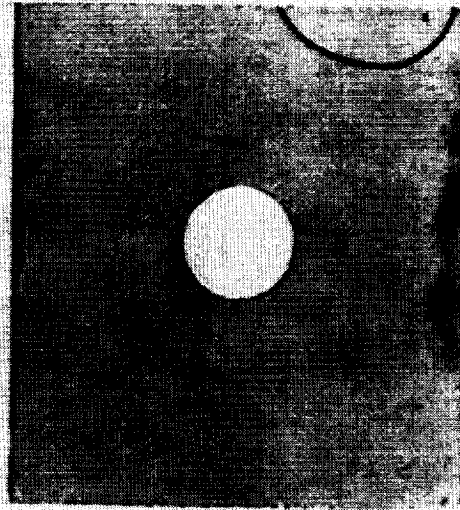
Textile

a)

LLS
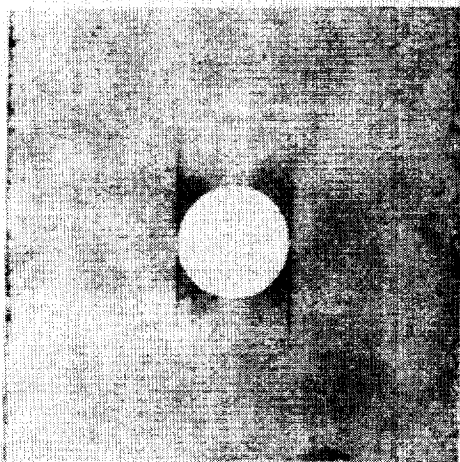
Tape
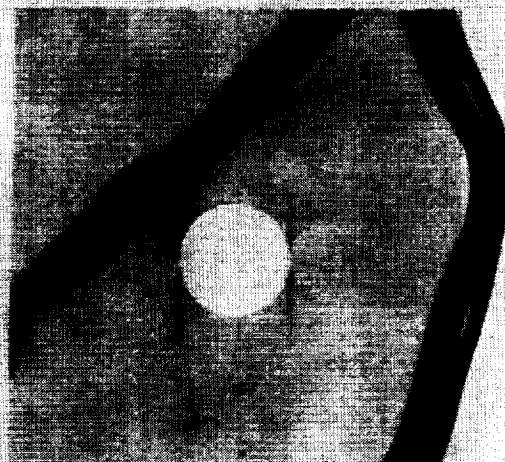
Textile

b)

Figure 21. Radiographs of textile and tape equivalents at 75% of ultimate failure stress with architectures corresponding to a) LSS, b) LLS, c) SLL and d) LLL.

39

SLL

Tape   Textile

c)

LLL
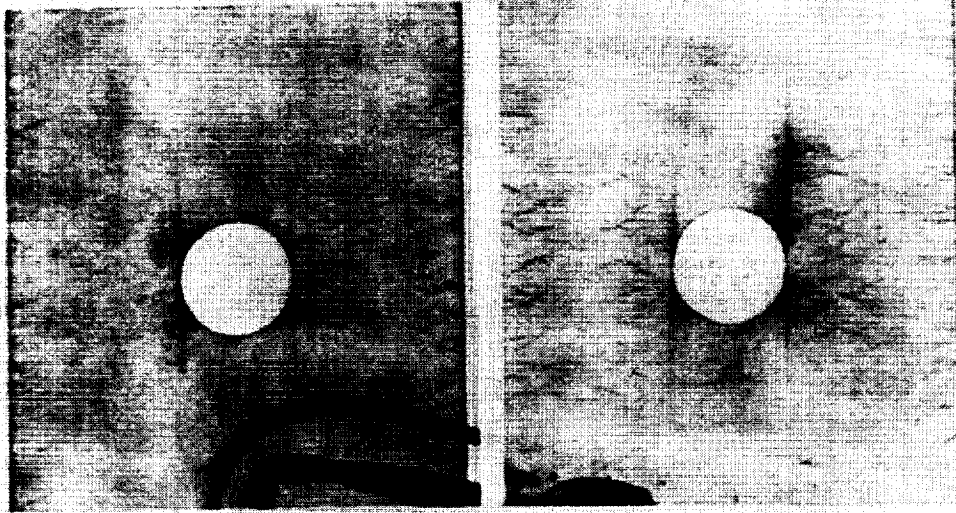
Tape   Textile

d)

Figure 21. (Continued).

Longitudinal Yarn

**Braider Yarn
Cracking**
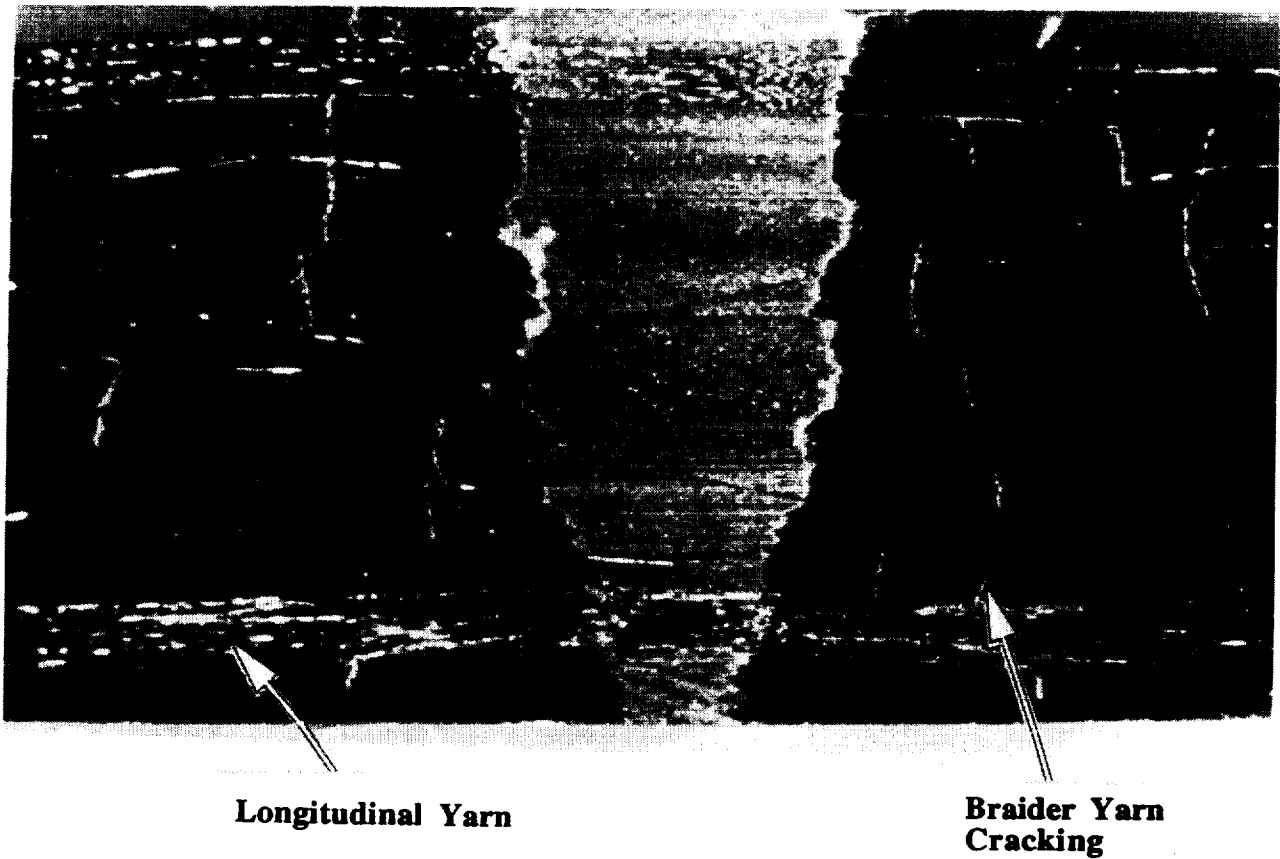
Figure 22. 45° section (Fig. 4) of a LSS notched coupon at 75% of failure stress looking
out from the inside of a hole along the braider yarn direction. Cracking in the braider
yarns is observed at the notch through the thickness similar to edge cracks of unnotched
coupons. The nominal thickness is 3.175 mm.

Figure 23. Transverse cross-section (Fig. 4) of a notched LLS textile coupon showing the location of the longitudinal crack identified at the hole edge (Fig. 21d). The photomicrograph shows that the longitudinal crack in yarn splitting. The crack is shown after grinding/polishing approximately 3 mm toward the load direction. The nominal thickness is 3.175 mm.
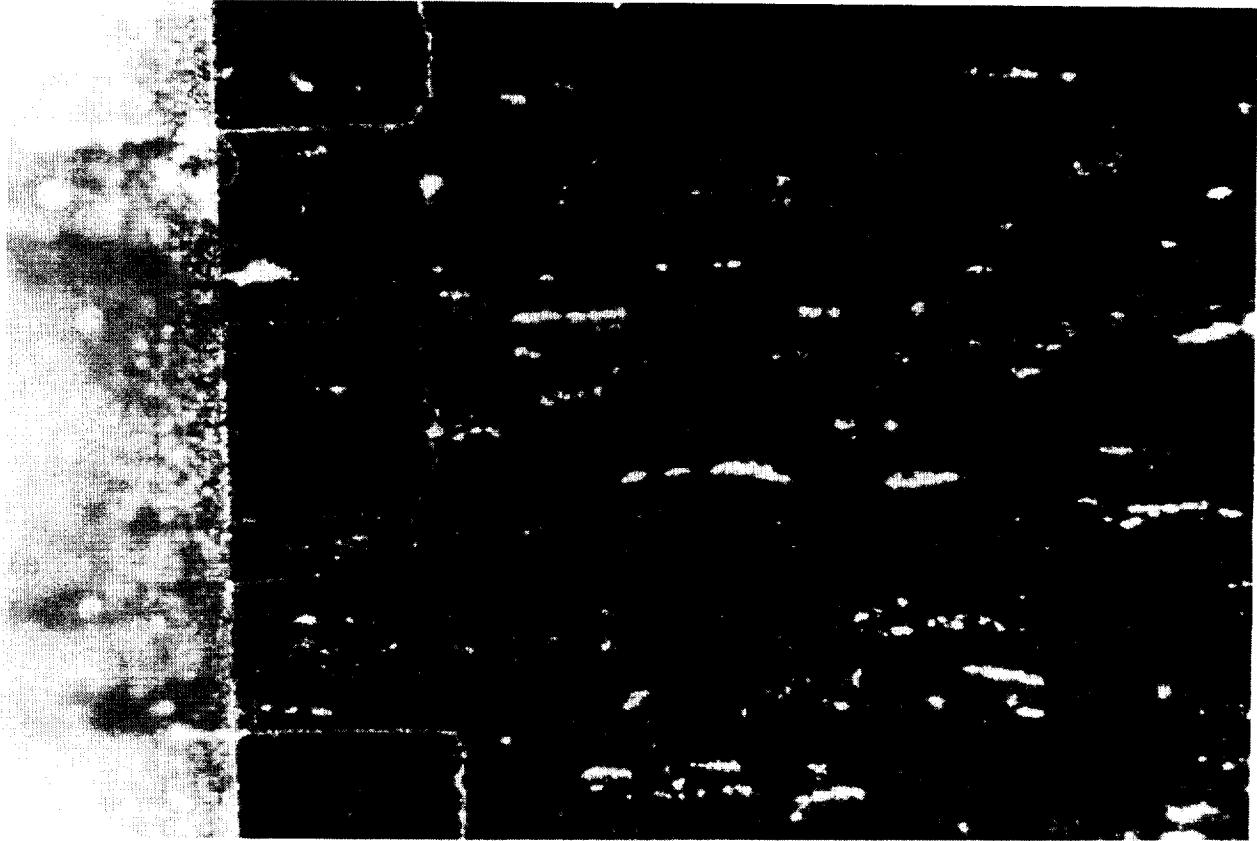
Figure 24. Transverse cross-section (Fig. 4) of a notched LLS tape equivalent coupon showing the location of the longitudinal cracks identified at the hole edge (Fig. 21b). The photomicrograph shows that the longitudinal crack is within the 0° layer and propagates to and along the ±45/0° interface.
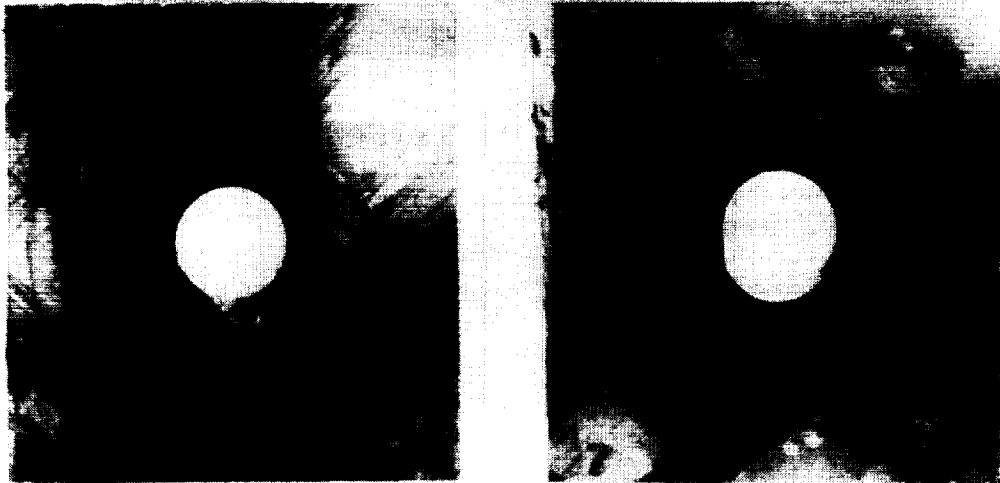
Figure 25. Radiographs of textile and tape equivalents at failure with architectures corresponding to a) LSS, b) LLS, c) SLL and d) LLL.

SLL

Tape **Textile**

c)

LLL
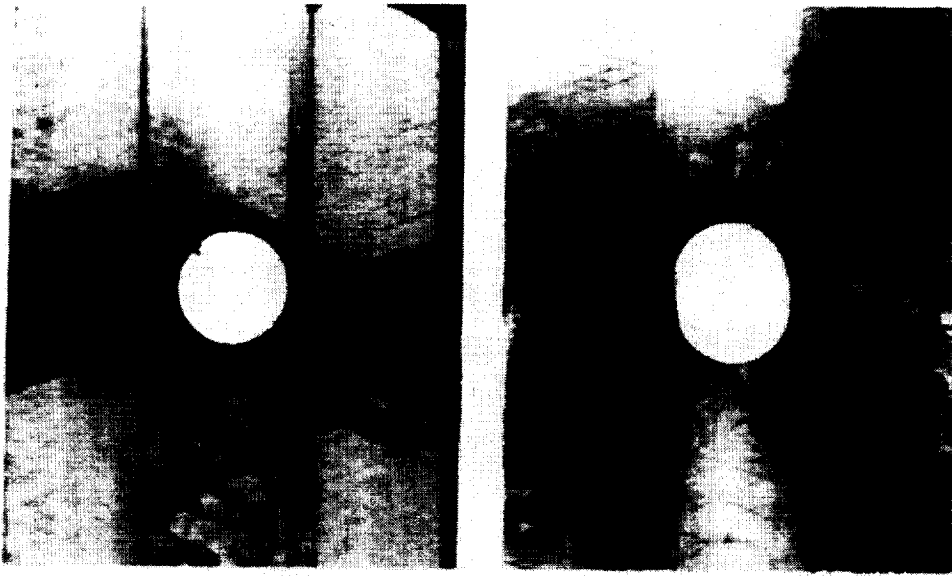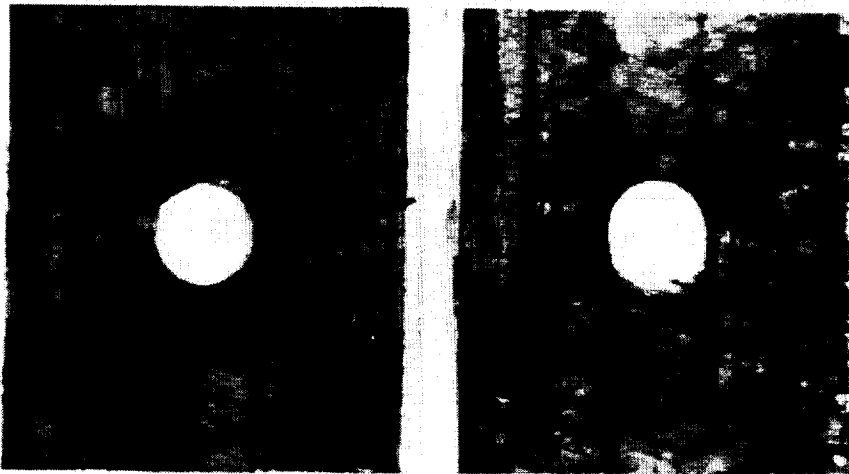
Tape **Textile**

d)

Figure 25. (Continued).

45

Figure 26. Longitudinal photomicrograph of an LSS unnotched coupon at failure. Extensive cracking in braider yarns and delaminations of the braider and longitudinal yarns are observed. The nominal thickness is 3.175 mm.
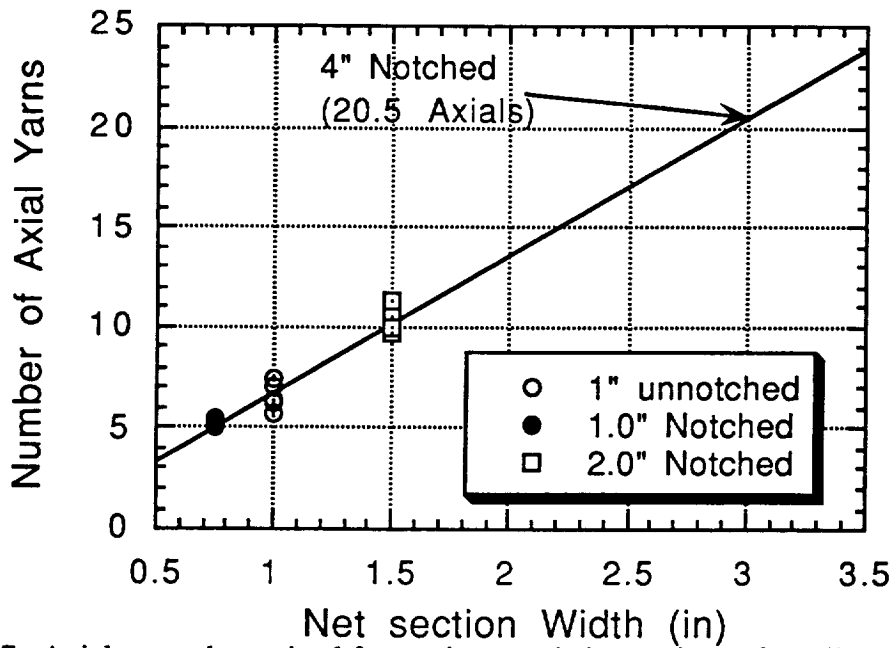
Figure 27. Axial yarns determined from microscopic inspections of tensile specimens. The number of longitudinals for the 4" notched specimens is found from extrapolation.
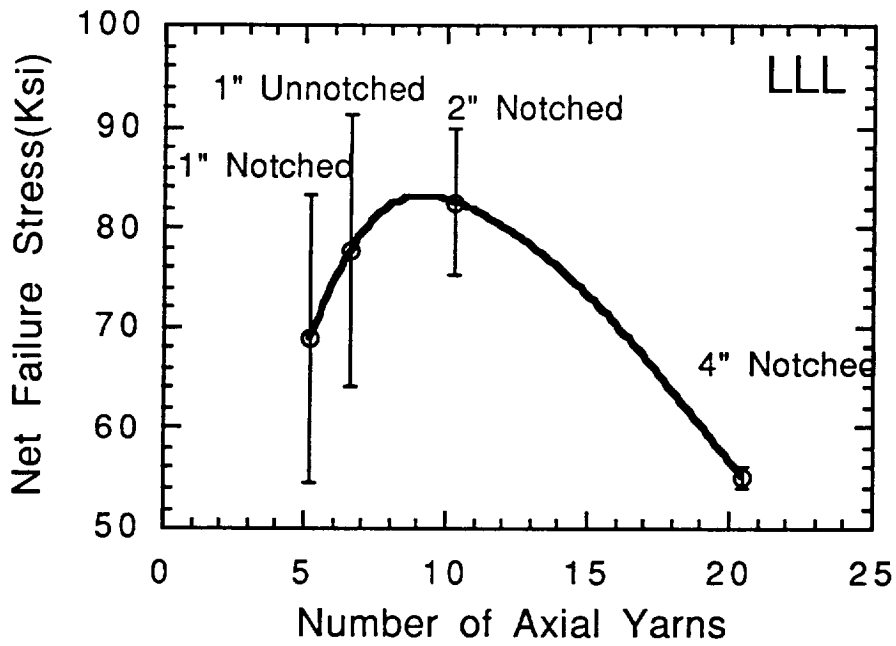
Figure 28. The competing sensitivities of notch size number of axial yarns suggesting that net section width of near 1.5" coupons should be minimum for LLL.

47

REPORT DOCUMENTATION PAGE

Public reporting burden for this collection of information is estimated to average 1 hour per response, including the time for reviewing instructions, searching existing data sources, gathering and maintaining the data needed, and completing and reviewing the collection of information. Send comments regarding this burden estimate or any other aspect of this collection of information, including suggestions for reducing this burden, to Washington Headquarters Services, Directorate for Information Operations and Reports, 1215 Jefferson Davis Highway, Suite 1204, Arlington, VA 22202-4302, and to the Office of Management and Budget, Paperwork Reduction Project (0704-0188), Washington, DC 20503.

1. AGENCY USE ONLY *(Leave blank)*	2. REPORT DATE June 1995	3. REPORT TYPE AND DATES COVERED Contractor Report

4. TITLE AND SUBTITLE

Effect of Open Hole on Tensile Failure Properties of 2D Triaxial Braided Textile Composites and Tape Equivalents

6. AUTHOR(S)

Timothy L. Norman, Colin Anglin, David Gaskin, and Mike Patrick

5. FUNDING NUMBERS

G NAG1-1381

WU 510-02-11-07

7. PERFORMING ORGANIZATION NAME(S) AND ADDRESS(ES)

West Virginia University
Department of Mechanical and Aerospace Engineering
Morgantown, WV 26507

8. PERFORMING ORGANIZATION REPORT NUMBER

9. SPONSORING / MONITORING AGENCY NAME(S) AND ADDRESS(ES)

National Aeronautics and Space Administration
Langley Research Center
Hampton, VA 23681-0001

10. SPONSORING / MONITORING AGENCY REPORT NUMBER

NASA CR-4676

11. SUPPLEMENTARY NOTES

Langley Technical Monitor: Clarence C. Poe, Jr.
Final Report

12a. DISTRIBUTION / AVAILABILITY STATEMENT

Unclassified - Unlimited

Subject Category 24

12b. DISTRIBUTION CODE

13. ABSTRACT *(Maximum 200 words)*

The unnotched and notched (open hole) tensile strength and failure mechanisms of two-dimensional (2D) triaxial braided composites were examined. The effect of notch size and notch position were investigated. Damage initiation and propagation in notched and unnotched coupons were also examined. Theory developed to predict the normal stress distribution near an open hole and failure for tape laminated composites was evaluated for its applicability to triaxial braided textile composite materials. Four fiber architectures were considered with different combinations of braid angle, longitudinal and braider yarn size, and percentage of longitudinal yarns. Tape laminates equivalent to textile composites were also constructed for comparison. Unnotched tape equivalents were stronger than braided textiles but exhibited greater notch sensitivity. Notched textiles and tape equivalents have roughly the same strength at large notch sizes. Two common damage mechanisms were found: braider yarns cracking and near notch longitudinal yarn splitting. Cracking was found to initiate in braider yarns in unnotched and notched coupons, and propagate in the direction of the braider yarns until failure. Longitudinal yarn splitting occurred in three of four architectures that were longitudinally fiber dominated. Damage initiation stress decreased with increasing braid angle. No significant differences in prediction of near notch stress between measured and predicted stress were weak for textiles with large braid angle. Notch strength could not be predicted using existing anisotropic theory for braided textiles due to their insensitivity to notch.

14. SUBJECT TERMS

Textile composites; Braids; 2D triaxial braids; Tensile strength; Notched coupons; Unnotched coupons; Damage initiation and growth

15. NUMBER OF PAGES

48

16. PRICE CODE

A03

17. SECURITY CLASSIFICATION OF REPORT	18. SECURITY CLASSIFICATION OF THIS PAGE	19. SECURITY CLASSIFICATION OF ABSTRACT	20. LIMITATION OF ABSTRACT
Unclassified	Unclassified		